University of California, San Diego
Institute of Geophysics and Planetary Physics

FINAL REPORT
Contract F44620-70-C-0099

sponsored by

Advanced Research Projects Agency
Air Force Office of Scientific Research
United States Air Force
Washington, D.C.

LOW FREQUENCY DISCRIMINANTS

ARPA Order No.   1618
Program Code No.   OF10
Contract Starting Date: 1 June 1970
Contract Expiration Date: 30 May 1971
Amount of Contract $106,963
Principal Investigator: Barry Block
                                        453-2000 Ext. 1735

September 28, 1971
La Jolla, California 92037
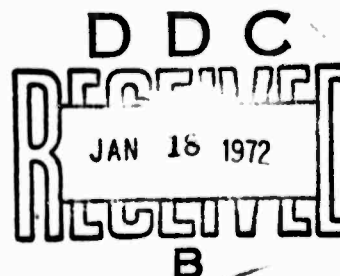
APPROVED FOR PUBLIC RELEASE; DISTRIBUTION UNLIMITED

41

DOCUMENT CONTROL DATA · R & D

(Security classification of title, body of abstract and indexing annotation must be entered when the overall report is classified)

1 ORIGINATING ACTIVITY *(Corporate author)*	2a. REPORT SECURITY CLASSIFICATION
Institute of Geophysics & Planetary Physics University of California, San Diego La Jolla, California 92037	UNCLASSIFIED
	2b. GROUP

3 REPORT TITLE

LOW FREQUENCY DISCRIMINANTS

4 DESCRIPTIVE NOTES *(Type of report and inclusive dates)*

Scientific.----------Final

5 AUTHOR(S) *(First name, middle initial, last name)*

Barry Block, Jay Dratler, Jr. Freeman Gilbert
James N. Brune William E. Farrell William A. Prothero, Jr.

6 REPORT DATE	7a. TOTAL NO. OF PAGES	7b. NO. OF REFS
28 September 1971	39	31

8a. CONTRACT OR GRANT NO.	9a. ORIGINATOR'S REPORT NUMBER(S)
F44620-70-C-0099	
b. PROJECT NO. 62701D	
c.	9b. OTHER REPORT NO(S) *(Any other numbers that may be assigned this report)* AFOSR - TR - 72 - 0082
d.	

10 DISTRIBUTION STATEMENT

Approved for public release;
distribution unlimited

11 SUPPLEMENTARY NOTES	12 SPONSORING MILITARY ACTIVITY
	Air Force Office of Scientific Research 1400 Wilson Boulevard (NPG) Arlington, Virginia 22209

13 ABSTRACT

   Broad band vertical and horizontal accelerometers were operated at the surface and at the 1,850 foot depth of a mine in New Jersey. In the seismic band of the vertical, the detection threshold on the surface and at 1,850 feet was M_s = 2.7 to 3.2 with a signal to noise ratio of 2 at 25 second periods.

   The horizontal was operated at the surface and showed much more noise than the vertical. However the digitally high passed records of the horizontal show a reduction in noise of almost a factor of 10 in the seismic band (50 - 20 second periods). This allows the horizontal surface instruments to have almost as good a filtered noise level as the surface vertical accelerometers.

   A catalog of all events taken in a continuous run of 6 months duration is in progress. All of this data is in digital form.

KEY WORDS

Broad band accelerometers
Broad band seismic instruments
Digitally filtered Seismic instruments
Seismic Detection
Wide band accelerometers

DD FORM 1 NOV 65 1473

LOW FREQUENCY DISCRIMINANTS

During the course of this research contract the following developments were made.

1. A quartz vertical accelerometer was operated at the 1,850 foot level of the New Jersey Zinc mine in Ogdensburg, New Jersey. This operation was carried out to compare the Lamont vertical accelerometer with the borehole deployable quartz instrument. The comparisons showed a somewhat lower noise level from the quartz instrument in the seismic prefilter bandwidth (see Technical Report dated March 1, 1971). However, during the mine operation a temperature controller problem was found and later corrected back at San Diego which lowered the noise level further.

2. The new vertical quartz accelerometer was operated at a surfact site at San Diego from January to July 1971. During this period data was digitized in the seismic normal mode and tidal channels. Several hundred events were recorded digitally. A student working for James Brune is preparing a catalog of all events during this period.

3. An analysis of small teleseismic events was made to determine detection thresholds. A paper on this is included (Prothero, et al.). A single vertical at San Diego has a detection threshold (signal to noise ratio of 2) for 25 second periods of M_s = 2.7 to 3.2 at Δ = 30°.

4. Several large earthquakes yielded earth normal mode data and one, the Colombian event July 31, 1970 gave many high Q overtone modes. The existence of the high Q's of these modes was unexpected. A paper on

this is included (Dratler, et al.). The average duty cycle for seeing normal mode excitation (20 db signal to noise) is about one day per month (Block, et al.).

5. The horizontal accelerometer was placed in operation in the same surface vaul as the verticals for several months. Many earthquakes were observed and digitized with these instruments. The horizontal showed a much higher noise level than the vertical in general. However, high pass digital filtering proved that the majority of this noise is below the seismic bandwidth (50-20 second periods) and that horizontal accelerometers can be operated on the surface at nearly the same signal to noise as verticals in the seismic band. A paper on this is included (Block, et al.).

6. Preparations were begun to waterproof the instruments for use in low noise sites perhaps including mine sites. A new portable data acquisition system was tested.

Fig. 2   Event 11 described in Table 1.

was dictated primarily by the shape of the ground noise spectrum, which has a minimum in amplitude between periods of 20 and 30 s.   This minimum may be inferred from the known decrease in noise amplitude with increasing period at shorter periods and seismic background noise data[5].   It is also shown in the data of Savino et al.[6].

The chief features of this instrument of importance to the seismic detection problem are: (1) a drift rate which is small so that a broad band position detector can be used; (2) a compact design with internal environmental control of temperature and pressure; (3) low ambient and instrumental noise level, totalling less than 5×10^{-23} g^2/c.p.h. (1.8×10^{-13} cm s^{-2}/ Hz) in the frequency band of interest (g is the local acceleration of gravity).
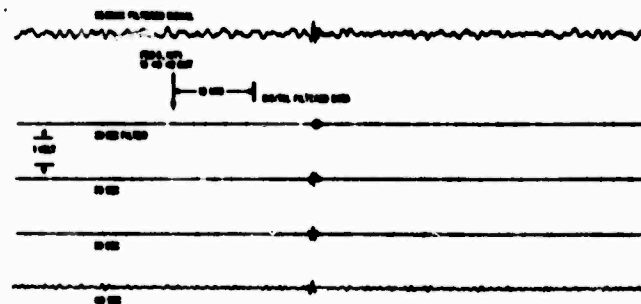
Fig. 3   Event 5 described in Table 1.

Our data were obtained at a surface site (vault depth of approximately 10 feet) which is next to the Miramar Naval Air Station in San Diego (32.88° N, 117.1° W).   This site is noisy at high seismic frequencies because of jet engine operation and traffic on a nearby freeway.   The site is, however, quiet at longer periods and the instrument response is sufficiently linear that no appreciable amount of high frequency energy is coupled down to low seismic frequencies.

The output is directly digitized at 1 s intervals and can be passed through narrow band digital filters.   Data taken at the Ogdensburg[7], New Jersey, mine site indicated a noise level approximately comparable with that described by Pomeroy et al.[3].   This instrument has the advantages of small size, low drift rate, and internal environmental control so that important difficulties with complicated vault construction and external environmental control are avoided.

Fig. 1 shows the response of the instrument to ground displacement at a given period in volts output per μm.   Seismic filter number 4 is the analogue filter.   The unfiltered broad band response is also shown and has the $1/T^2$ roll-off characteristic of an accelerometer with flat response to acceleration— T is the period.   At very long periods, the $1/T^2$ term becomes small and the effect of the gravity gradient predominates.

Surface Wave Detection with a Broad Band Accelerometer

WE report preliminary results of a study to determine the capability of a broad band vertical accelerometer to detect surface waves from small earthquakes.   The instrument uses a quartz fibre in torsion and capacitive position sensing[1].   It was designed as a low noise, low drift broad band accelerometer, and has produced data on Earth normal mode excitation after earthquakes (5 to 40 cycle h^{-1}, ref. 2).   For this study, the output was modified by an active filter to copy the response of Pomeroy et al.[3] and Molnar et al.[4].   Such a response does not use the wide band aspects of this instrument and the shape
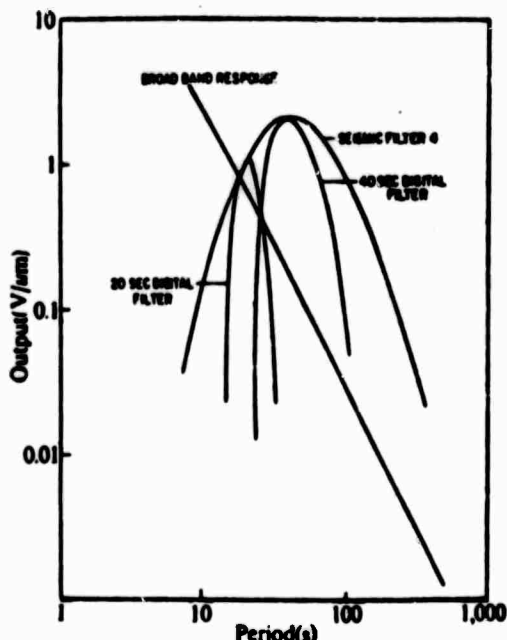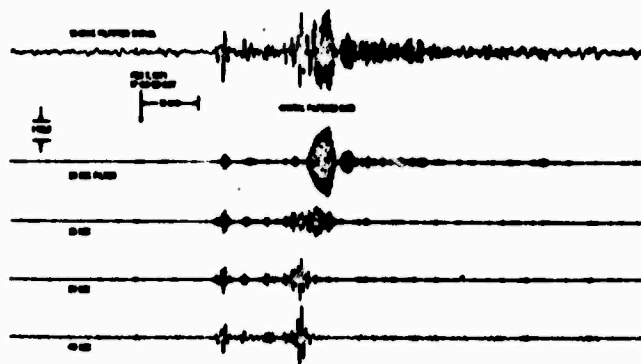

Fig. 1   Response of the accelerometer to ground motion in volts of output per μm of ground motion.   The digital filters shown are peaked at 20 s and 40 s, with bandwidths of 0.02 Hz.   The digital filters, peaked at 25 s and 30 s, have almost identical frequency responses.   The difference in the widths of the 20 s and 40 s filters shown is due to the inverse dependence of frequency and period.

Table 1 The Events Described in Figs. 2, 3, 4 and 5

Event	M_B	M_S	M_S (30°)	Epicentral distance Δ (degrees)	h (km)	I.D.	Region
11	5.2	5.3	4.6	77.7	53	LASA	Tonga Island Region
5	PDE reports not yet available.						
9	4.8	4.1	3.9	41.4	43	LASA NOAA PDE	Northern Easter Island, Cordillera
17	4.3	3.5	3.2	44.0	33	LASA	Andreanoff Island, Aleutians

The body wave magnitudes (M_B) are as determined by LASA or NOAA PDE reports as indicated. The surface wave magnitudes (M_S) were determined from our records using the surface wave magnitude relation of Gutenberg[10], where $M_S = \log_{10} A + 1.66 \log_{10} \Delta + 1.82$. A is the maximum horizontal ground movement (μm) observed for surface waves with periods ~20 s. The vertical and horizontal motions are assumed equal. M_S (30°) is the surface wave magnitude of each event normalized to a distance of 30°.

Figs. 2, 3, 4 and 5 are computer generated plots of the seismic filter output for several teleseismic events. The digitized output has been digitally band pass filtered by several symmetric convolution filters with bandwidths of 0.02 Hz and centre frequencies corresponding to periods of 20, 25, 30 and 40 s. The response to ground displacement for the 20 and 40 s digital filters is shown in Fig. 1. Table 1 lists the magnitudes, depths and distances of the events shown. The surface wave magnitude of an earthquake at 30° which would produce 20 s surface waves of the same amplitude is also given for each event. Event number 17 of Fig. 5 has a signal to noise ratio of approximately 5 on the 25 s filtered record; it would correspond to an event with surface wave magnitude 3.2 at 30°. The amplitude of the noise on the 25 s filtered trace at this site (15 nm) corresponds to the amplitude of an event with a surface wave magnitude of 2.4 (20 s) at a distance of 30°. Other filtering methods may be used to decrease the detection threshold even more[6,9].

An event with $M_B = 5.2$ (LASA) at a distance of 77.7° is shown in Fig. 2. Several body wave phases are clearly visible; and for smaller magnitude events, only the surface wave arrivals are apparent. Fig. 4 shows an event with $M_B = 4.8$

(LASA and NOAA PDE) at a distance of 41.4° which shows a large mantle wave excitation. The digital filters increase the signal to noise ratio for the surface wave train in all events. The 25 s filter seems to show the largest signal to noise ratio in general.

These results indicate that it is possible to achieve a relatively low surface wave detection threshold in a simple surface vault in the presence of large short period seismic noise using the Block–Moore quartz torsion accelerometer. The digital data recording system has also been found invaluable, as it provides a large dynamic range. Direct digitization also allows flexibility and speed in data reduction. Further tests will be carried out to determine site variations in ground noise amplitude and detection threshold.

We thank R. A. Haubrich for help, and researchers at the Ogdensburg Mine of the Lamont-Doherty Geophysical Observatory, where the instrument comparisons were made. This research was supported in part by the Advanced Research Projects Agency of the Department of Defense and was monitored by the Air Force Office of Scientific Research.

W. PROTHERO
J. DRATLER
J. BRUNE
B. BLOCK

Institute of Geophysics and Planetary Physics,
University of California,
La Jolla,
California 92039

Fig. 4 Event 9 described in Table 1.
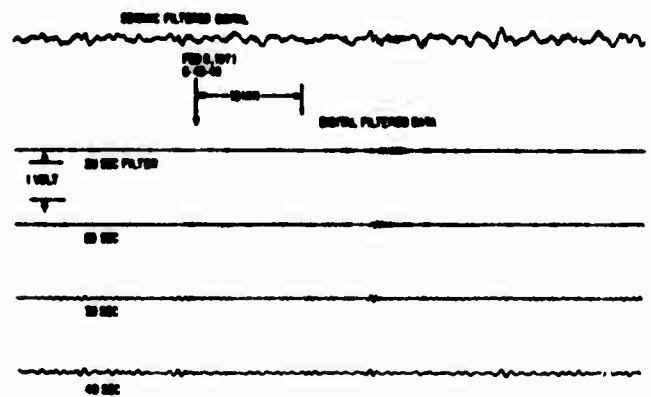
Fig. 5 Event 17 described in Table 1.

[1] Block, B., and Moore, R. D., J. Geophys. Res., 75, 1493 (1970).
[2] Block, B., Dratler, J., and Moore, R. D., Nature, 226, 343 (1970).
[3] Pomeroy, P. W., Hade, G., Savino, J., and Chander, R., J. Geophys. Res., 74, 3295 (1969).
[4] Molnar, P., Savino, J., Sykes, L. R., Liebermann, R. C., Hade, G., and Pomeroy, P. W., Nature, 224, 1268 (1969).
[5] Haubrich, R., Low Level Earth Motion, Final Report of Air Force Contract AF49(638)-1388 (1969).
[6] Proc. ARPA Meeting on Seismic Discrimination, Woods Hole (July 1970).
[7] Block, B., Low Frequency Discriminants, Technical Report of ARPA Contract F44620-70-C-0099 (1970).
[8] Klauder, J. R., et al., Bell Systems Tech. J., 39 (July 1960).
[9] LaCoss, R. T., A Large Population LASA Discriminant Experiment, MIT Lincoln Laboratory Technical Note 1969-24 (1969).
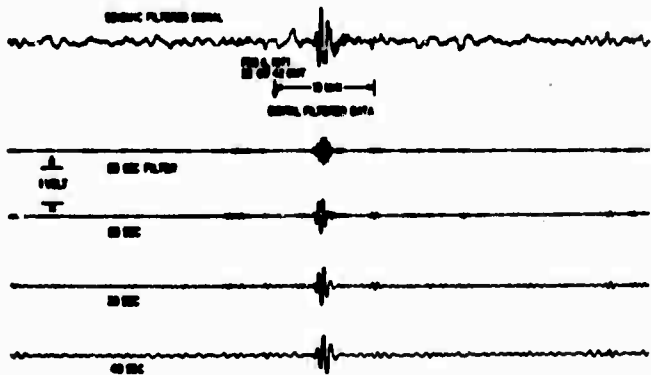[10] Gutenberg, B., Bull. Seismol. Soc. Amer., 35 (1945).

High-Q Overtone Modes of the Earth

J. Dratler, Jr., W. E. Farrell, B. Block and F. Gilbert

(Received 1971 March 18 in revised form)

Summary

Overtone modes of free oscillation of the Earth have been observed with two instruments at two separate locations after the Colombian earthquake of July 31, 1970. Certain overtones persisted with a signal-to-noise ratio as high as 20 db for 50 hr after the origin time. Some spheroidal radial overtones (modes of type $_nS_0$) were found to have Q's near 1000, about three times the typical Q of a fundamental mode ($_0S_l$). Multiplet centre frequencies and Q's were measured for several overtones, with good agreement between the two stations.

Introduction

Excitation of the free oscillations of the Earth by large earthquakes has been observed for a decade. The low frequency normal modes of the Earth were first observed after the Chilean earthquake of 1960 (1)-(3). Normal mode activity has been measured after several subsequent earthquakes with a variety of instruments (4). In these early investigations, the frequencies and decay rates of the fundamental modes in the frequency band 1–20 cph were studied. Spheroidal fundamental modes from $_0S_0$ to $_0S_{30}$ were observed often. Typical Q's for these fundamentals were estimated to be roughly 300, except for $_0S_0$, whose Q is several thousand.

For several reasons, the spectrum of overtone modes (modes of type $_nS_l$, where $n > 0$) is not as well known. The overtones, in general, are not as strongly excited as the fundamentals, and instrument and earth noise in the data hamper their identification. The overtone sequences, having successively higher and higher starting frequencies, are only present in the part of the frequency domain where the lines are dense. Thus, it is difficult to identify the overtone modes by their frequency alone. Deep focus earthquakes excite the overtone modes more strongly than shallow earthquakes, but large, deep events are rare.

Alsop & Brune (5) have discussed the overtone modes excited by a 7¾ magnitude event at a depth of 543 km, which occurred on the Peru-Bolivia border in 1963. They used phase velocities as well as frequencies to identify modes from a 6 hr 45 min record. Second through fifth overtones in the frequency range 15–36 cph were observed, but some of these were later re-identified by Derr (4).

There are two prerequisites for observations of free oscillations with a good signal-to-noise ratio. One is a sensitive, low-noise seismic intrument with good response at low frequencies, operating at a low-noise site; and the other is a large earthquake to

1

excite the overtone oscillations. In the present study two instruments using extremely sensitive capacitative position sensing, a modified LaCoste Romberg survey gravimeter (6), and the Block–Moore Quartz-fibre accelerometer (7), satisfied the first prerequisite. Fortune supplied the latter, in the form of the Colombian Earthquake of July 31, 1970. This earthquake (origin time 17:08:05·4 GMT July 31, 1970, epicentre 1·5° S, 72·6° W, near the Peru–Colombian border), had magnitudes $M_s = 6·8$ and $m_b = 7·1$, was 651 km deep, and excited the overtone oscillations strongly. Useful data were obtained for about 80 hr after the first arrival with the Block–Moore instrument, and for slightly more than 67 hr with the LaCoste instrument. Overtone modes were identified from the decay rates, as well as calculated eigenfrequencies, and good agreement was found between the two instruments located several hundred kilometers apart.

Data

In the past year, numerous recordings of free oscillations generated by relatively small earthquakes have been made (8). The earthquake discussed here is the first large, deep focus event we have observed. Time series from the event were taken with the two different vertical accelerometers at two locations. The modified LaCoste gravimeter was located in Payson, Arizona, at the Tonto Forest Seismological Observatory (34·24° N. Lat, 111·34° W. Long.). The Block–Moore instrument was located at the IGPP Camp Elliott, California, field station (32·88° N. Lat., 117·1° W. Long.), about 13 miles north-east of San Diego. The distances of the two stations from the earthquake epicentre were $\Delta_E = 54·13°$ for Camp Elliott and $\Delta_P = 50·85°$ for Payson. Haubrich (9) has studied the background earth noise at the two locations, using data from the same two instruments, and has found the noise level in the 4–20 cph band to be about $10^{-24} g^2$/cph.

Outputs from both instruments were passed through active electronic filters (7) with gains of 40 db in the passband from 1 to 30 cph and 40 db/decade rolloffs. Filtered output from the Block–Moore instrument was recorded digitally on magnetic tape at a sampling interval of 1 s. Filtered output from the LaCoste instrument was printed digitally on paper tape at a sampling interval of 12 s, after additional low-pass filtering to avoid aliasing.

For studying the data from the Block–Moore instrument, a record beginning 5 hr and ending 80 hr after the earthquake origin time was used. The first few hours of the data were discarded because the large Rayleigh waves saturated the instrument electronics. This constituted no serious loss, as even more data was intentionally ignored in the subsequent analysis. The record was terminated at 80 hr after origin time as spectra of records taken after this time seemed to show no features appreciably above the noise level. The raw data was interpolated across a few instrumental artifacts, high-pass filtered to remove the tides, and finally low-pass filtered and decimated to a Nyquist frequency of 60 cph.

A part of the Fourier power spectrum of the entire 75 hr record is shown in Figs 1(a) and 2(a). For clarity, the region from 4 to 12·3 cph is shown in Fig. 1, and that from 12·3 to 21 cph in Fig. 2. The theoretical positions of the fundamental spheroidal modes $_0S_l$ are shown at the top of each figure. With the exception of $_0S_{22}$, all the fundamental normal modes in Fig. 1(a) from $_0S_{10}$ to $_0S_{25}$ can be identified. In addition to the fundamentals, other lines are observed with signal-to-noise ratios greater than 10 db. These lines, some of which are marked in Figs 1(a) and 2(a), are overtone modes of free oscillation. The most striking example is the line on the low-frequency shoulder of the fundamental $_0S_{20}$. While it is well resolved from the fundamental, it has a signal strength 15 db above the jitter in the Fourier spectrum, and thus is clearly not noise. From theoretical considerations, it is identified as the sixth overtone of unit angular order $_6S_1$.

FIG. 1. Fourier power spectra from 4 to 12.3 cph of data taken with the Block-Moore vertical accelerometer at Camp Elliot, California, after the Colombian earthquake of 1970 July 31. The 0 dB point is 10^{-24} g^2/cph. (a) Spectrum of time series from 5 to 80 h after earthquake origin time, with theoretical positions of fundamental ($_0S_l$) earth normal modes. Some overtone lines are marked with vertical strokes. (b) Spectrum of time series from 20 to 80 h after origin time, with theoretical positions(10) of the radial overtones $_nS_0$. Lines are identified from theory as described in the text. Note decay of fundamentals relative to certain overtones. (c) Spectrum of time series from 30 to 80 h after origin time. Note persistence of high-Q overtones.
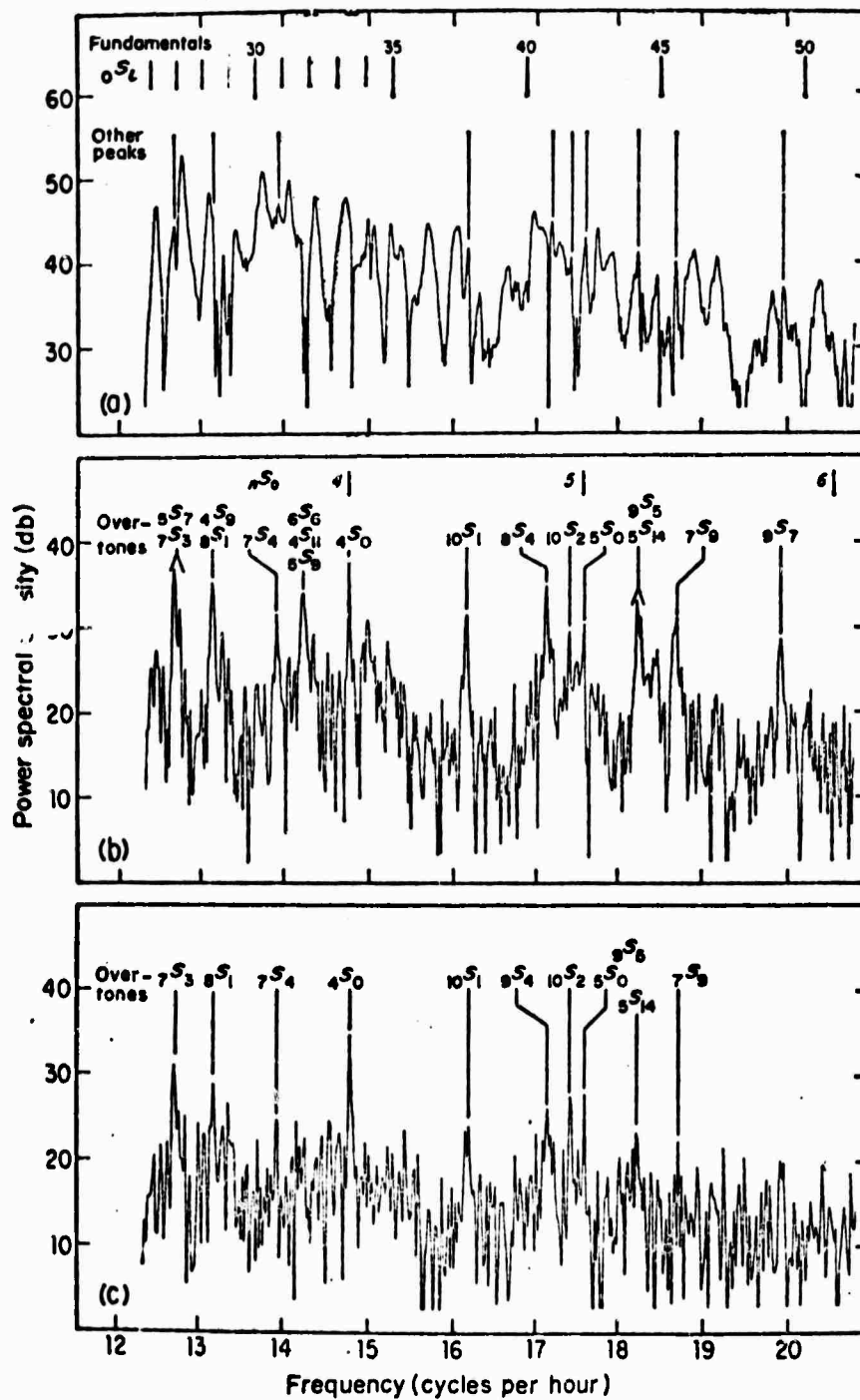
FIG. 2. Continuation of spectra of Fig. 1 from 12·3 to 21 cph. Fall-off with increasing frequency is due to electronic and digital filters used in processing the data.

Part (b) of Figs 1 and 2 shows the Fourier power spectrum of the record from 20 to 80 hr after the earthquake origin time. Here, the fundamental modal lines have decayed considerably, while the overtone lines marked in Figs 1(a) and 2(a) still have quite a high signal-to-noise ratio. Only the lower-frequency fundamental normal modes, marked in Fig. 1(b), are now identifiable. The theoretical frequencies of the radial overtones $_nS_0$ are marked in the figures, while the observed overtone lines are identified as described below.

In part (c) of Figs 1 and 2, the Fourier power spectrum of the data from 30 to 80 hr after the earthquake origin time is shown. In these spectra, the fundamental normal modes have decayed away almost entirely. The persistance of certain overtone lines after the decay of the fundamentals indicates that they have a Q significantly larger than 300, the approximate Q of the fundamentals. In fact, after m cycles, the energy of a simple harmonic oscillator with quality factor Q decreases to a factor of $\exp(-2\pi m/Q)$ of its initial value. For a typical fundamental mode with frequency 10 cph and $Q = 300$, the expected decay is about 10 db in 10 hr. The fundamentals shown do, in fact, have a decay of this order, but some of the overtones are considerably more persistent, suggesting Q's two or three times greater than 300. Signal-to-noise ratios for the final 50-hr record (part (c)) are as high as 20 db, even more than a day after the origin time.

To measure the actual Q's of the persistent lines, a 'time-lapse' series of spectra was made. Segments of the original record from 10 to 30, 20 to 40, 30 to 50, 40 to 60, and 50 to 70 hr after the earthquake origin time were separately Fourier transformed. Since the length of these sections was constant and much greater than the period of any mode of interest, the peak of each line occurred at the same Fourier frequency in each spectrum, and phases of the decaying oscillations were unimportant. Thus, the standard expression for the decay of the power spectral peak from spectrum to spectrum was valid:

$$\frac{P_K}{P_{K-1}} = e^{\frac{-\omega_0 T}{Q}} \text{ or } lnP_K = lnP_0 - \frac{K2\pi f_0 T}{Q} \text{ for } Q \gg 1. \tag{1}$$

Here, P_K is the height of the Kth 'time-lapse' spectral peak, $\omega_0 = 2\pi f_0$ is the angular frequency of the given mode, and $T = 10$ hr is the time elapsed between the beginnings of the consecutive records. The Q for each observed high-Q line was calculated from a linear least-squares fit of lnP_K to KT, according to the above formula. The frequency and Q measured for each high-Q overtone line are shown in Table 1.

Table 1

Observed frequencies and Q's of overtone lines

Mode	Frequency (cph)		Q^*	
	Elliot	Payson	Elliot	Payson
$_3S_0$	9·0294	9·0151	672	704
$_4S_0$	14·7833	14·7819	1173	1156
$_5S_0$	17·5941	17·5979	938	927
$_6S_0$		20·6690		
$_4S_1$		7·1686		
$_6S_1$	10·3379	10·3373	613	700
$_8S_1$	·13·1541	13·1562	420	380
$_{10}S_1$	16·1592	16·1568	696	574
$_4S_4$	·8·5603	8·5634		
$_4S_5$	9·7276	9·7367		
$_4S_6$	10·8377	10·8371		
$_4S_7$	11·7724	11·7806		

* All Q values have standard errors between 10 and 20 per cent except for $_4S_0$, which has 10 per cent standard error.

9

Quite similar results were obtained with the data from the modified LaCoste gravimeter at Payson, Arizona. The digital record at Payson began at 0200 GMT August 1, 1970, about 9 hrs after the earthquake origin time, and ended 67 hr 13 min later. A Fourier power spectrum of the data from 10 to 70 hr after the origin time, after removal of tides, digital filtering and decimation to a Nyquist frequency of 30 cph, is shown in Figs 3(a) and 4(a). The similarity of this spectrum to that of Figs 1(a) and 2(a) is obvious. Differences in the apparent excitation levels of the various modes can be explained on the basis of the radiation pattern of the source. A particularly striking example of this is the fundamental mode $_0S_{22}$, which appears strongly excited in the Payson record and is non-existent in the Camp Elliott record. We infer that Camp Elliott was nearly on a node of the $_0S_{22}$ mode for this source.

Parts (b) and (c) of Figs 3 and 4 are spectra of the intervals 20–70 and 30–70 hr after the origin time. Again there is good correlation with the Camp Elliott results. The high signal-to-noise ratio for the radial overtone series, even 30 hours after the earthquake, is quite remarkable. It can be ascribed to the quality of the site and low instrument noise.

A 'time-lapse' series of spectra was made for the Payson data. Portions of three of these 'time-lapse' spectra are presented in Fig. 5. In the first spectrum, the strongly excited fundamentals tend to obscure the more weakly excited overtones. However, as the series progresses, the low-Q modes die away, while the high-Q overtones persist. The Q's were determined for the lines with highest signal-to-noise ratio, as described above. The results are given in Table 1. For those modes whose Q's were reasonably high, there was quite good agreement between the Q values measured at Camp Elliott and those measured at Payson.

The power spectral density for all figures is given in decibels above 10^{-24} g^2/cph, which is roughly the Brownian motion noise level of the two instruments. It should be noted, however, that the actual instrumental noise is somewhat higher than this theoretical limit, particularly for the Block–Moore accelerometer. The total noise level is best estimated by a careful examination of the jitter in the spectra. For instance, in Fig. 1(a), the noise level appears to be about 35 db between 4 and 6 cph and less than 30 db above 7 cph. In Figs 1(b) and (c), the noise level estimated from the jitter is about 25 db. Such estimates include instrumental noise and ground noise.

Also, the figures are not corrected for the response of the electronic and digital filters used in data processing. This introduces errors in the absolute spectral densities as read from the figures which are normalised to the peak of the combined filter response. These errors, however, are small and systematic. At 4 cph, the figures read 1 db low; at 6 cph, the figures are correct; above 6 cph, the figures read increasingly low until they are 6 db low at 20 cph. The standard error in the calibration at the peak is ±1 db.

Modal identification

The primary criterion for the identification of a given line was its frequency. Since theoretical calculations of the eigenfrequencies have become both rapid and accurate (10), it was possible to compare the measured line frequency to its calculated value with some confidence. When a given line occurred at a frequency well separated from those of neighbouring lines, and when the observed frequency matched the calculated frequency closely, this was considered sufficient identification of the line.

Often, however, there were several calculated eigenfrequencies in the neighbourhood of an observed peak, so that identification by frequency alone was ambiguous. In these cases it was nearly always possible to identify the line unambiguously from its Q. One of the outputs of our theoretical calculation of the eigenfrequencies from an earth model is a partition of the potential energy of a mode into elastic shear energy, elastic compressional energy, and gravitational energy. Since shear is far

Fundamentals
$_0S_i$

Other peaks

(a)

Power spectral density (db)

$_nS_0$

Overtones

Fundamentals
$_0S_i$

(b)

Overtones

Fundamentals
$_0S_i$

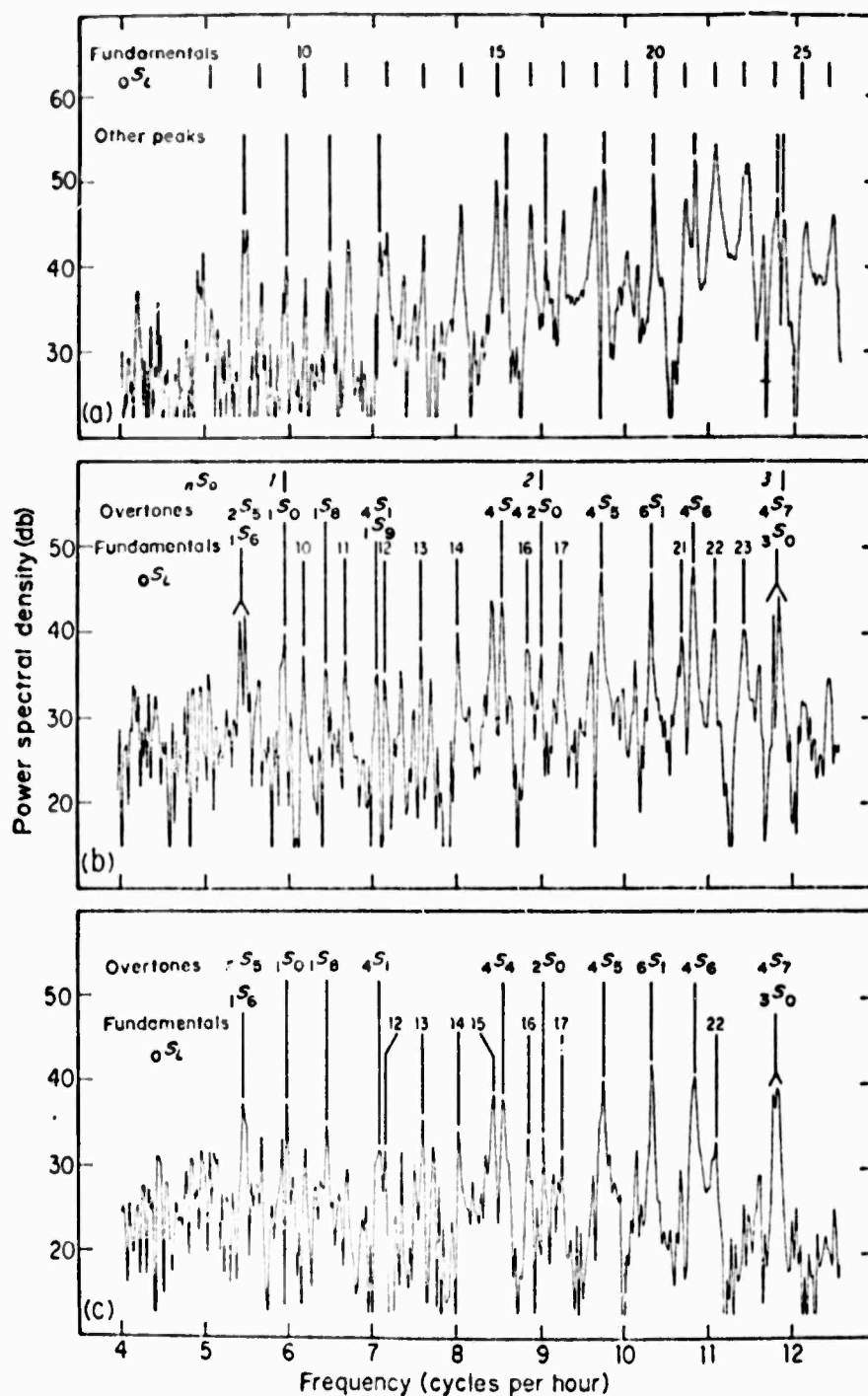(c)

Frequency (cycles per hour)

FIG. 3. Fourier power spectra from 4 to 12·5 cph of data taken with modified LaCoste-Romberg survey gravimeter at Payson, Arizona, after Colombian earthquake of 1970 July 31. The 0 dB point is 10^{-24} g²/cph. (a) Spectrum of time series from 10 to 70 h after earthquake origin time, with theoretical positions of fundamental ($_0S_i$) earth normal modes. Overtone lines are marked with vertical strokes. (b) Spectrum of time series from 20 to 70 h after origin time, with theoretical positions of radial overtones $_nS_0$. Lines are identified from theory as described in text. Note similarity to Fig. 1(b). (c) Spectrum of time series from 30 to 70 h after origin time. Note similarity to Fig. 1(c).
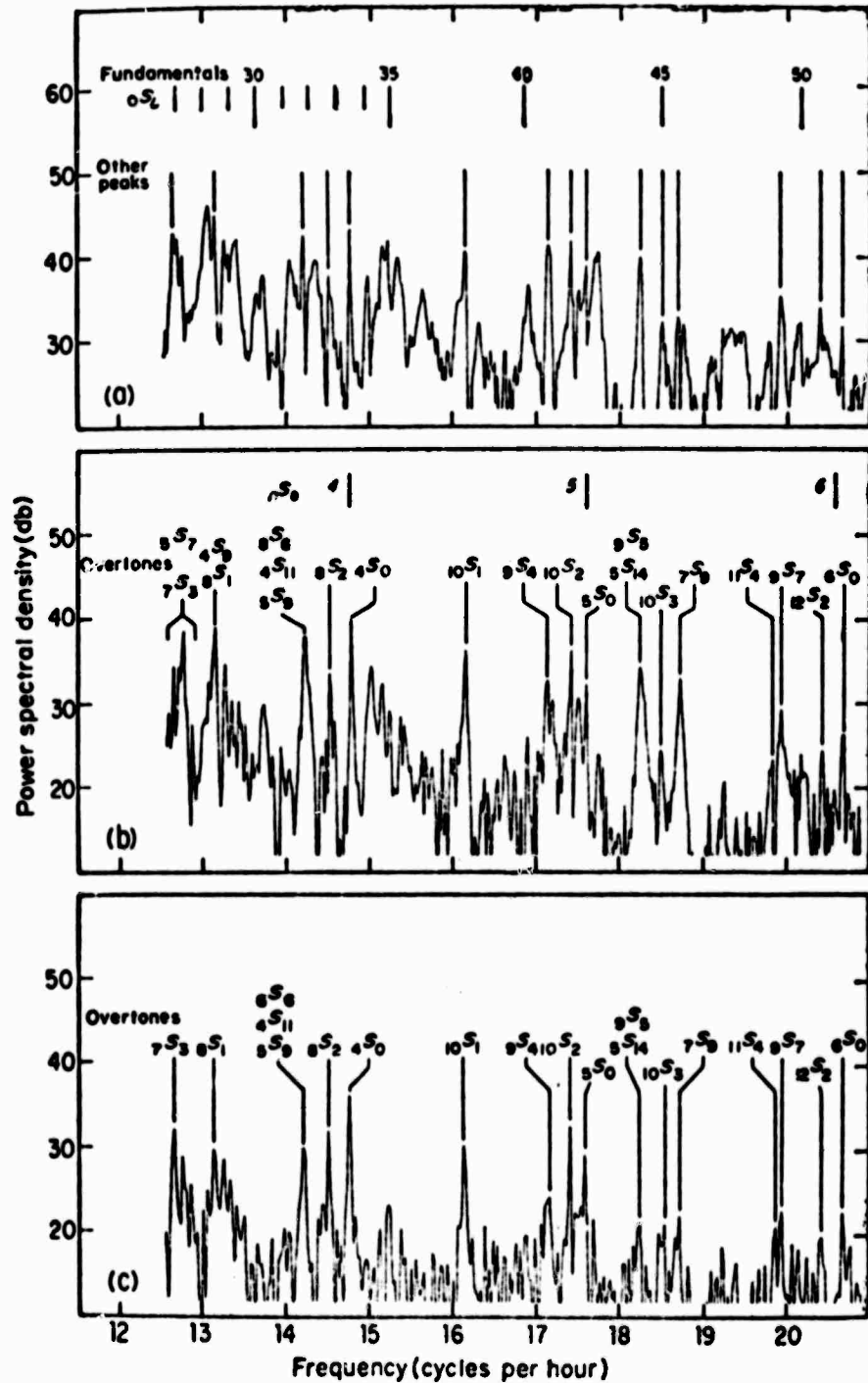
Fɪɢ. 4. Continuation of spectra in Fig. 3 from 12·5 to 21 cph. Fall-off with increasing frequency is due to electronic and digital filters used in processing the data. Note similarity to Fig. 2.
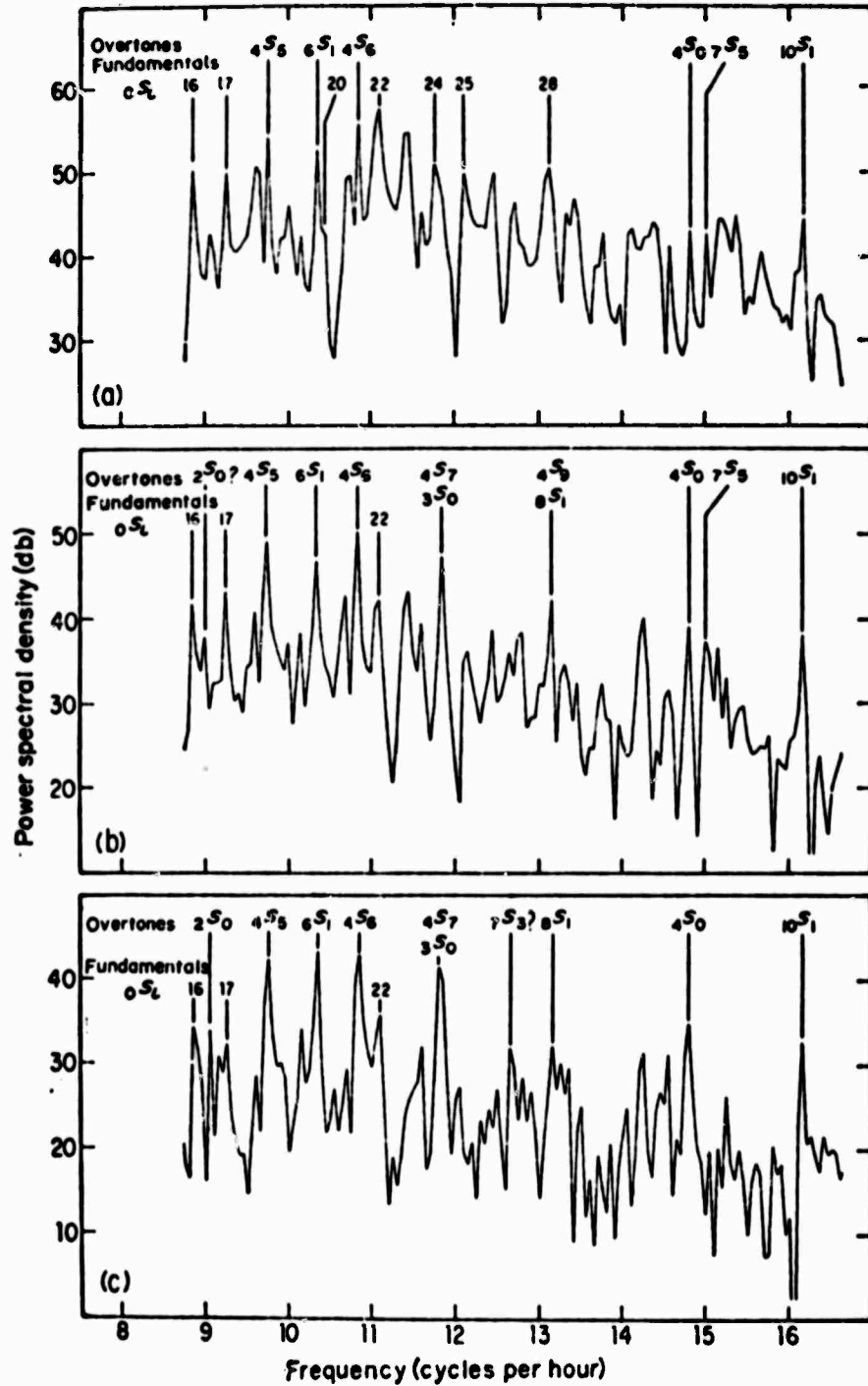
FIG. 5. ' Time-lapse ' Fourier power spectra of data taken at Payson. The 0 dB point is 10^{-24} g²/cph. (a) Spectrum from 10 to 30 h after origin time. Note strong fundamental excitation. (b) Spectrum from 20 to 40 h after origin time. Note dominance of overtones. (c) Spectrum from 30 to 50 h after origin time. Note decay of fundamentals and persistence of high-Q overtones.

13

more dissipative than compression (11), and since no energy stored in the gravitational field is lost, the Q of a given mode is largely determined by its fractional shear energy. Modes with high fractional shear energy have low Q, and vice versa. In cases where identification of a mode was ambiguous on the grounds of frequency alone, comparison of the observed Q with the calculated fractional shear energy of all candidate modes usually served to identify the line.

As a final aid in line identification, a rough theoretical calculation of the relative modal amplitudes was made. By means of a computational shortcut recently developed (12), it is possible to calculate rapidly the spectrum excited by a given earthquake source function. The location (epicentre and depth) of the Colombian earthquake was obtained from the U.S. Coast and Geodetic Survey cards, while the fault plane attitude and direction of slippage were guessed. The relative amplitudes · calculated from this source mechanism agreed fairly well with the observed relative amplitudes for the known lines. These amplitude calculations were then used to corroborate identifications based on calculated Q's in regions where frequency identifications alone were not sufficient.

Results

The centre frequencies observed at each station for the identifiable overtone multiplets are listed in Table 1. For some of these overtones, the measured Q is also listed. However, this is done for only those lines for which discrepancy between the two measurements is less than 20 per cent.

It should be emphasized that not all the overtone free oscillations have high Q. Figs 1–4 show many overtone lines which, although having greater Q than the fundamentals, do not persist from part (b) to part (c). These lines have higher Q than the fundamentals, but less than the radial overtones. They have Q's in the range 500–700. According to theory, there are also many overtones whose Q is of the order of 300, or the Q of the fundamentals. These lines are not observable, however, as they are initially obscured by the highly excited fundamentals and decay at the same rate, thus remaining obscured.

A word of caution is needed about the Q measurement. The representation of the normal mode eigenfunctions as spherical harmonics degenerate with respect to azimuthal degree is only a zeroth-order approximation. As has been shown (13), when the ellipticity and rotation of the earth are considered, the single lines of the zeroth order theory become multiplets of $2l + 1$ lines, where l is the angular order of the spherical harmonic. The existence of this multiplet structure makes it impossible, in general, to measure the Q of an observed mode unless the individual lines in the multiplet can be resolved.

Suppose, for example, that an attempt is made to determine the Q of a modal multiplet by measuring the line width. The quantity of interest is really the line widths of the individual lines in the multiplet, which are related to the decay rates. If these individual lines cannot be resolved, only the line width of the multiplet as a whole can be measured. This, however, is not related directly to a physical decay rate, as it depends on how the various subsidiary lines in the multiplet are excited. It is of interest only as an upper bound to the line widths of the subsidiary lines. Thus, in general, Q values determined from unresolved multiplets are merely lower bounds to the Q of the individual lines. A good example of this phenomena is the line $_0S_{23}$ in Fig. 1(a), whose strange shape is undoubtedly due to differential excitation of the 47 lines in the multiplet.

Although the observations of Q above were made in the time domain, and not in the frequency domain, this reasoning still holds. In the time domain, the analogue of the phenomenon of line broadening due to multiplet splitting is the phenomenon of beating between different components of the multiplet. A careful consideration of

the effects of beating leads to the previous result, namely, that a Q measured from the decay of an unresolved multiplet is only a lower bound to the actual Q (14).

Of course, the above considerations do not apply to the radial overtones $_nS_0$, as they are singlets. As for the modes in the $_nS_1$ series, which are really triplets, the splitting has been estimated to be quite small for the modes observed here. The effective 'Q', or $f_0/\Delta f$, of this splitting is greater than 10 (4), so that the much lower measured Q of the multiplet is a fairly good estimate of the individual line Q. Thus, the observed Q values given in Table 1 for the $_nS_0$ and $_nS_1$ nodes should be rather accurate.

Conclusions

The free oscillations of the Earth excited by the Colombian earthquake of July 31, 1970 have been observed with two different instruments at two separate locations. In addition to the fundamental spheroidal normal modes, the data contain many spheroidal overtunes, some never previously observed. Analysis of the data shows that the unit angular order overtones, as well as the $_nS_0$ radial overtones, have Q s of the order of 1000, three times higher than the typical fundamental Q. Other modal lines of high Q were observed, but the Q's could not be accurately determined due to signal-to-noise problems.

It is important to stress that, in the event of a large deep earthquake, these high-Q free oscillations can be observed with any sensitive low-frequency accelerometer. In this study, the modified LaCoste gravimeter with electrostatic position sensor, a relatively old instrument, and the Block–Moore accelerometer, a new instrument, were used. The vital elements of any such study are continuity of observation and digital recording recording of data. In fact, in the classic study of Ness, Harrison & Slichter (1961) of the Chilean earthquakes of May 1960 (1), the presence and persistence of the high-Q mode $_4S_0$ was observed, but it was not identified. This was achieved with an instrument whose noise level in the normal mode region was more than 30 db above that of our intrsuments.

With the earthquake of the same size ($M_s \simeq 8\cdot 2$) today, an enormous wealth of free oscillation data could be obtained. Modal splitting could be resolved and compared with theoretical predictions. Many new overtones could be observed, and the Q's of these overtones, with splitting resolved, could be accurately determined. All these data, used as input to inversion techniques, could supply a better picture of the internal structure and dissipation mechanisms of the Earth.

Acknowledgments

Institute of Geophysics and Planetary Physics,
University of California,
San Diego, La Jolla,
California, 92037

References

(1) Ness, N. F., Harrison, J. C. & Slichter, L. B., 1961. Observations of the free oscillations of the earth, *J. geophys. Res.*, **66**, 621–629.

(2) Benioff, H., Press, F. & Smith, S., 1961. Excitation of the free oscillations of the earth by earthquakes, *J. geophys. Res.*, **66**, 605–619.

(3) Alsop, L. E., Sutton, G. H. & Ewing, M., 1961. Measurements of Q for very long period free oscillations, *J. geophys. Res.*, **66**, 2911–2915.

(4) Derr, J. S., 1969. Free oscillation observations through 1968, *Bull. seism Soc. Am.*, **59**, 2079–2099.

(5) Alsop, L. E. & Brune, J. N., 1965. Observations of free oscillations excited by a deep earthquake, *J. geophys. Res.*, **20**, 6165.

(6) Block, B. & Moore, R. D., 1966. Measurements in the Earth mode frequency range by an electrostatic sensing and feedback gravimeter, *J. geophys. Res.*, **71**, 4361–4375.

(7) Block, B. & Moore, R. D., 1970. Tidal to seismic frequency investigations with a quartz accelerometer of new geometry, *J. geophys. Res.*, **75**, 1493–1505.

(8) Block, B., Dratler, J. & Moore, R. D., 1969. Normal modes from a 6·5 magnitude earthquake, *Nature*, **226**, 343–349.

     Dratler, J., Jr., Normal modes generated by small earthquakes (part of Ph.D. thesis, in preparation)

(9) Haubrich, R. A., 1971. Origin and characteristics of microseisms at frequencies below 140 cycles per hour, *Monographies de l'UGGI*, in press.

(10) Gilbert, F., 1970. Normal mode eigenfrequency calculations (to appear in *Methods of computational Physics*).

(11) Anderson, D. & Archambeau, C., 1964. The anelas' city of the earth, *J. geophys. Res*, **69**, 2071–2084.

(12) Gilbert, F., 1971. Excitation of the normal modes of the Earth by earthquake sources, *Geophys. J. R. astr. Soc.*, in press.

(13) Dahlen, F. A., 1968. The normal modes of a rotating elliptical Earth, *Geophys. J. R. astr. Soc.*, **16**, 329–367.

     Dahlen, F. A., 1969. The normal modes of a rotating elliptical Earth-II. Near resonance multiplet coupling, *Geophys. J. R. astr. Soc.*, **18**, 397–436.

(14) Gilbert, F. & Backus, G., 1965. The rotational splitting of the free oscillations of the Earth--2, *Rev. Geophys.*, **3**, 1–9.

REPORT ON A NEW BROAD BAND

VERTICAL ACCELEROMETER

(presented at ARPA Conference
Woods Hole, July 1970)

by

Barry Block

Institute of Geophysics and Planetary Physics
University of California, San Diego
La Jolla, California

17

REPORT ON A NEW BROAD BAND VERTICAL ACCELEROMETER

Several years ago at the Institute of Geophysics and Planetary Physics, La Jolla, a program was begun to build a new generation of acceleration measuring instruments. This program has as its goal the creation of broad band instruments whose noise and drift properties are understood. It was felt that the lack of broad band accelerometers was hampering the growth of some theoretical branches of geophysics and that the narrow band data gathered was preventing a clear physical picture of many phenomena from emerging. With due consideration of the design achievments made in the past, we felt that technology had progressed to the point where a fundamental review was necessary. Our basic guide lines were taken to be

1. Tidal to seismic frequencies should be measurable by the same instrumental design.

2. Drift and other noise sources should be controlled to a level where interesting geophysical information can be obtained from tidal to seismic frequencies.

3. Linear response (i.e., freedom from non-linear processes) should be inherent in the mechanical structure of the instrument.

4. Internal calibration over frequencies from DC to seismic should be possible. The advent of phase sensitive detection allows the use of broad-band position detectors with a sensitivity far in excess of what is needed and which have extremely low detector noise. These detectors allow a new design freedom in the choice of the mechanical system. It is now no longer necessary to

make long period mass-spring systems to get the requisite overall gain of the accelerometer. In fact, there are many advantages to making a simple mechanical structure with a free period from about 1/2 to 1 second. Such a simple structure can be found which has all its higher modes well separated in frequency from the fundamental mode and which has small non-linear coupling from the higher modes to the fundamental mode. This structure is shown in Figs. 1 and 2.

The mass is cantilevered on a horizontal stretched monolithic quartz fiber which is in torsion to provide the restoring torque. It should be pointed out that this design can be used as a horizontal accelerometer merely by turning it on its side and letting the mass hang down. (Fig.2) In use for the past year as a vertical accelerometer and gravimeter, one model has given an upper bound to its drift rate of 10^{-10}g/day. In other words, full scale earth tides can be run for a year without rezeroing. Several other models have shown similar low drift. This low drift rate is achieved through processes described in a recent paper[1].

Instrument noise coming from temperature and barometric changes are controlled directly at the instrument and not in a large vault as has been the custom. Fig. 3 shows the mechanical setup of the instrument. The mass spring system is sealed at 10^{-7} mmHg pressure in a stainless steel gold O-ring sealed tank (8 inch diameter). This inner tank is suspended from the lid of an outer (9 inch diameter) aluminum tank sealed at 1 mmHg by conventional rubber O-rings. In operation, all adjustment apparatus is removed from direct contact with the inner tank. This double container provides protection from direct barometric effects. The thermostat is

-2-

wound on the outer container and a thermal feedback system has been designed to provide thermal control which in practice does not drift more than a microdegree per day over many months of use.

It should be pointed out that no particular effort has been made to minaturize this instrument and considerable progress is possible if a smaller version is needed. The static calibration and linearization is done by tilting the instrument about two perpendicular axes and the dynamic calibration by using an electrostatic force applied to the mass. The calibration can be carried out to the percent level in an unambiguous way. The instrument has been operated simultaneously with three outputs each 10 V full scale.

a. Tidal channel: Operated at 2×10^{-7} g full scale. Flat from DC to 4.8 cph, 20 db/decade drop after 4.8 cph.

b. Earth normal mode channel: Gain of 1 from DC to 1 cph, gain of 100 in band 1 - 30 cph, 40 db/decade drop at frequencies higher than 30 cph; operated at 2×10^{-9} g full scale in pass band 1 - 30 cph.

c. High frequency filter channel: A variable gain channel with pass band centered at 40 second period whose response mimics the response of the Lamont long period seismometers.

With this background in mind, I would like to show you some (with a free period of 1/2 second and Q=15) results from the first model/in the earth mode frequency band which we have somewhat arbitrarily called 1 - 30 cph. I will restrict my remarks to data drawn from the earth mode frequency band and leave the seismic results to be discussed by James Brune

-3-

In the first year of operation, we have recorded about two dozen magnitude 6.0 or larger earthquakes. These earthquakes show considerable earth mode (1 - 30 cph) excitation which can extend over many hours. Fig. 4 shows the earth mode filter record/taken during the magnitude

/(channel b above)

6.5, 246 km deep earthquake in the New Hebrides on October 13, 1969[2]. It is important to note the time scale on this figure. The background contains the earth tides and we see that the earthquake excitation lasts for nearly twelve hours in this fr quency band. A number of Rayleigh waves can be seen and a detailed look at an expanded time scale shows many phenomena of interest to the seismologist. The power spectrum of the earthquake is shown in Figs. 5, 6 and 7. The 0-db point is 1×10^{-24} g^2/cph. The ambient noise is also shown on these figures and is taken directly from the preceding record without any visible earthquakes. This ambient noise is the sum of the site noise and instrumental noise. This particular instrument has been found to operate at its Brownian limit by cross-correlation with another instrument but this cross-correlation was not carried out at this particular setup. The normal modes begin to clearly appear at about 8 cph and show at least 20 db signal to noise at frequencies above this. The spectra are shown up to 75 cph and again there is considerable power spectral energy up to these frequencies.

Fig. 8 shows a magnitude 7.5, 20 km deep earthquake at Sumatra

/ in the earth mode filter (channel b above).

on November 21, 1969 / The beginning of the event was off scale at the gain used and the data collection was interrupted some 18 hours later by a site power failure. There is considerable excitation still visible even after 18 hours. The power spectra are shown in Figs. 9 and 10

-4-

(again 0-db is 1×10^{-24} g^2/cph). The signal to noise ratio exceeds 20 db above 8 cph. The power spectra of many other earthquakes have been obtained and each one has shown its own distinctive spectral features.

It should be pointed out that over the last year, the duty cycle for seeing low order earth normal mode excitation is about one day per month. This is a great improvement over the previous rate of observations. The large amount and good quality of data gathered will certainly provide a great impetus to theoretical investigation of source mechanisms[3].

A second vertical accelerometer has been recently completed and is undergoing its initial tests. It has several new features such as a Q = 250 for low Brownian motion noise level and small stray capacity to ground to increase the signal to noise level. This second vertical instrument is being operated in the same vault as the first instrument and a series of cross correlation tests are planned for the pair.

A horizontal version of this basic design is being developed by Jay Dratler and is contemplated to have the same outputs as the vertical instruments.

In conclusion, the drift, temperature control and barometric control problems seem to have been solved for this instrument. It is internally calibratable, linear, and has a broad-band output. The first instrument has given earth normal mode excitation for earthquakes of magnitude 6.5 and greater with good signal to noise. Such instrumentation can now provide the broad band output necessary for the next generation of seismic investigation.

-5-

22

REFERENCES

1. Block, B., and R. D. Moore, Tidal to seismic frequency investigations with a quartz accelerometer of new geometry, *J. Geophys. Res.*, *75*, 1492 (1970).

2. Block, B., J. Dratler, R. D. Moore, Earth normal modes from a 6.5 magnitude earthquake, *Nature*, *226*, 343-344 (1970).

ILLUSTRATIONS

fiber mounting yoke

center clamp

gravitating mass

Figure 1

fiber tension spring

quartz fiber

line up pins

fiber tension adjust screw

end clamp

compression ring

rotation clamp

tension spring spacer

fiber tension adjust lever

25

signal lead

capicitor plates

ceramic stando

1 mil tungsten
signal lead

fiber mounting yoke

quartz fiber

gravitating mass

capacitor plate electrostatic shields

capicitor plate yoke

plink stopper

bellows connecting plate

parallel motion spring (upper)

spring stiffeners

capacitor plate support

copper counter weight

quartz capacitor plate spacer

signal ground

capacitor plate bolt

parallel motion spring (lower)

26

Figure 2

insulation

motor

outer can

thermostat windings

inner can

tilting platform

Figure 3

27

NEW HEBRIDES EARTHQUAKE

06:56 GMT OCT 13, 1969
18.9°S 169.3°E
$M_s = 6.5$ h = 246 km

1 HOUR

Figure 4

28

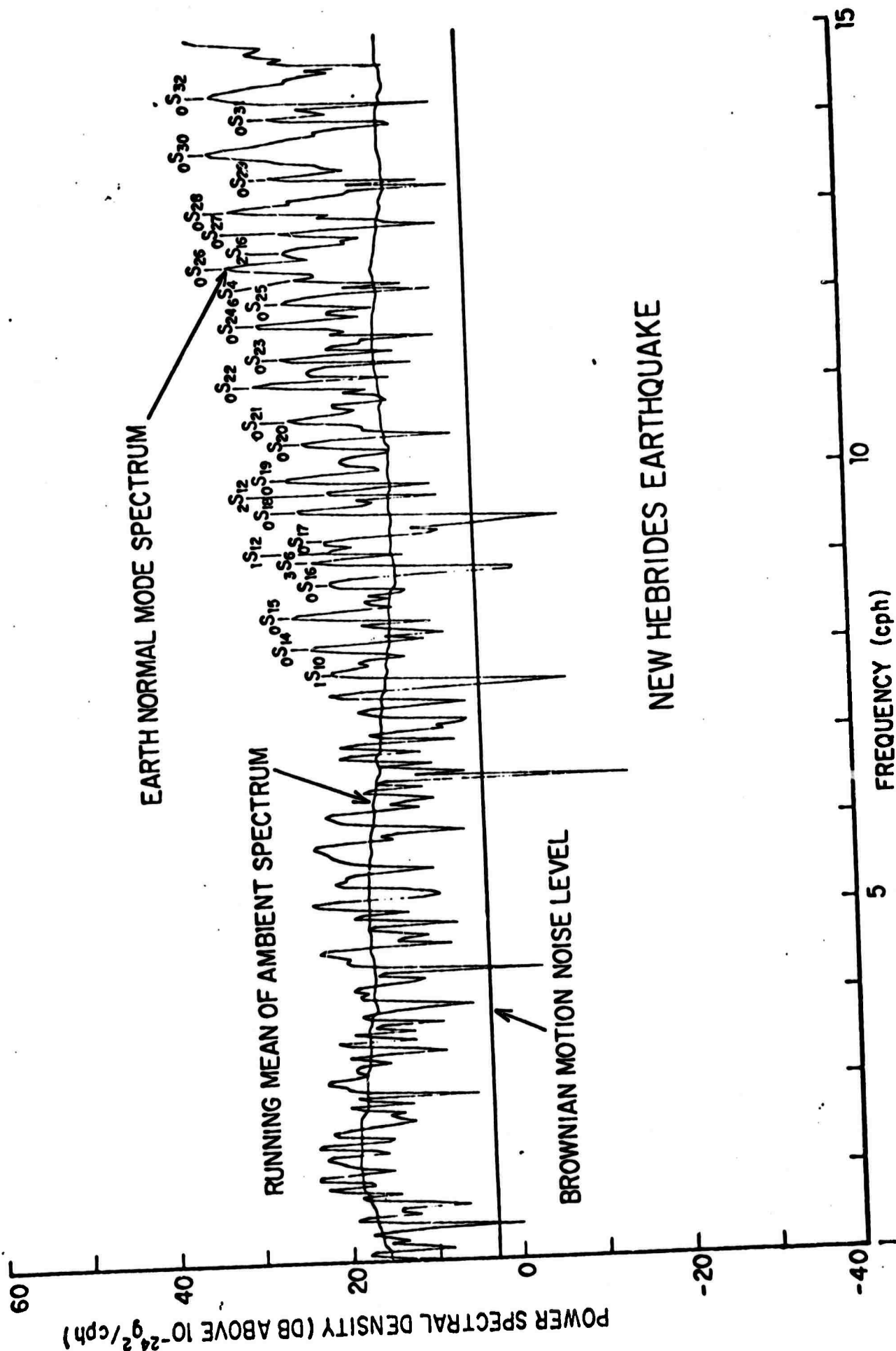POWER SPECTRAL DENSITY (DB ABOVE $10^{-24}g^2$/cph)

FREQUENCY (cph)

EARTH NORMAL MODE SPECTRUM

RUNNING MEAN OF AMBIENT SPECTRUM

BROWNIAN MOTION NOISE LEVEL

NEW HEBRIDES EARTHQUAKE

Figure 5

NEW HEBRIDES EARTHQUAKE

Figure 6

NEW HEBRIDES EARTHQUAKE
06:56 GMT OCT 13, 1969
18.9°S 169.3°E
$M_b=6.5$ h=246 km

EARTHQUAKE SPECTRUM

AMBIENT SPECTRUM WITH
RUNNING MEAN

POWER SPECTRAL DENSITY (DB ABOVE $10^{-24} g^2/cm$)

FREQUENCY (cph)

Figure 7

31
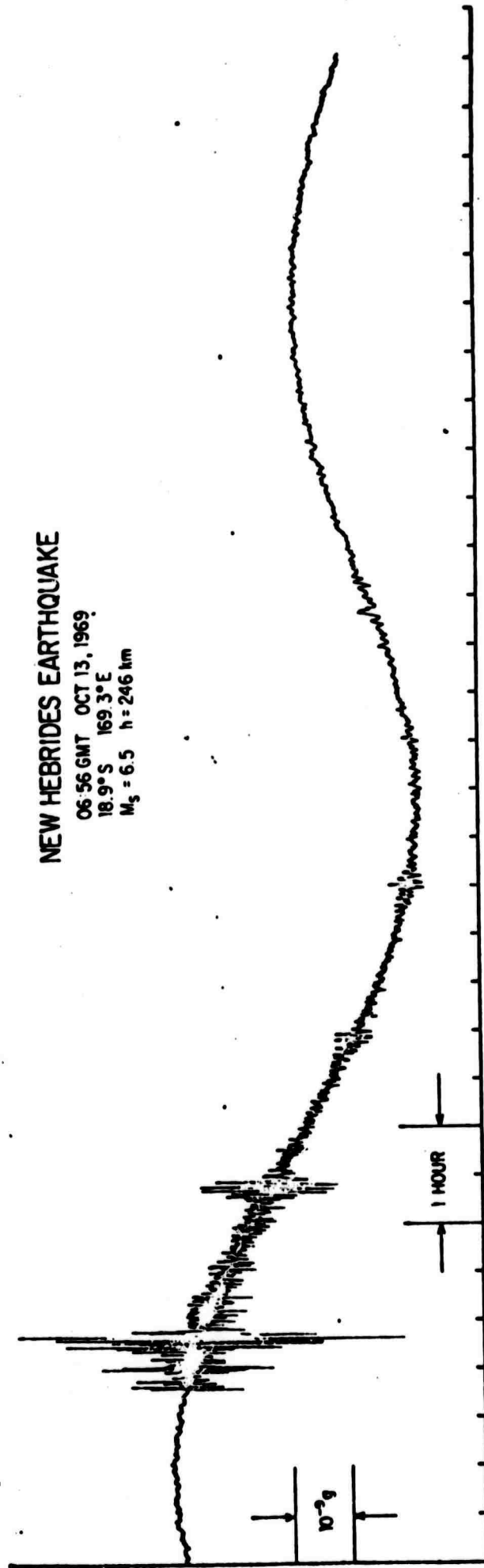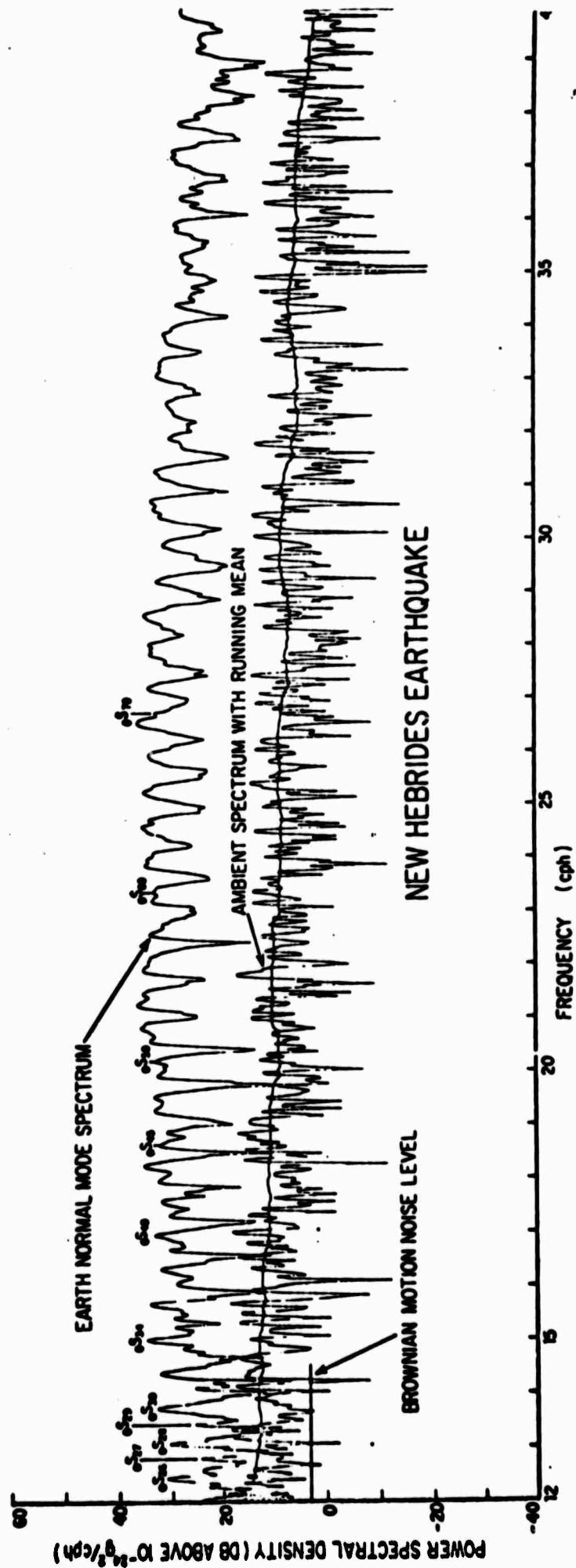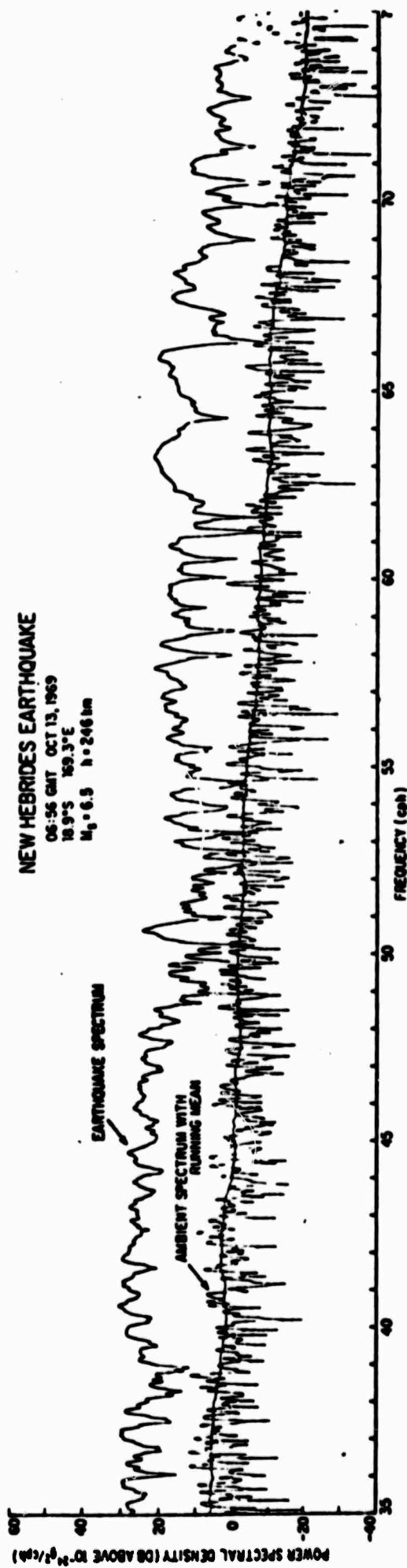
SUMATRA EARTHQUAKE
02:06 GMT NOV 21,1969
2.1°N 94.6°E
M_s = 7.5 h = 20 km
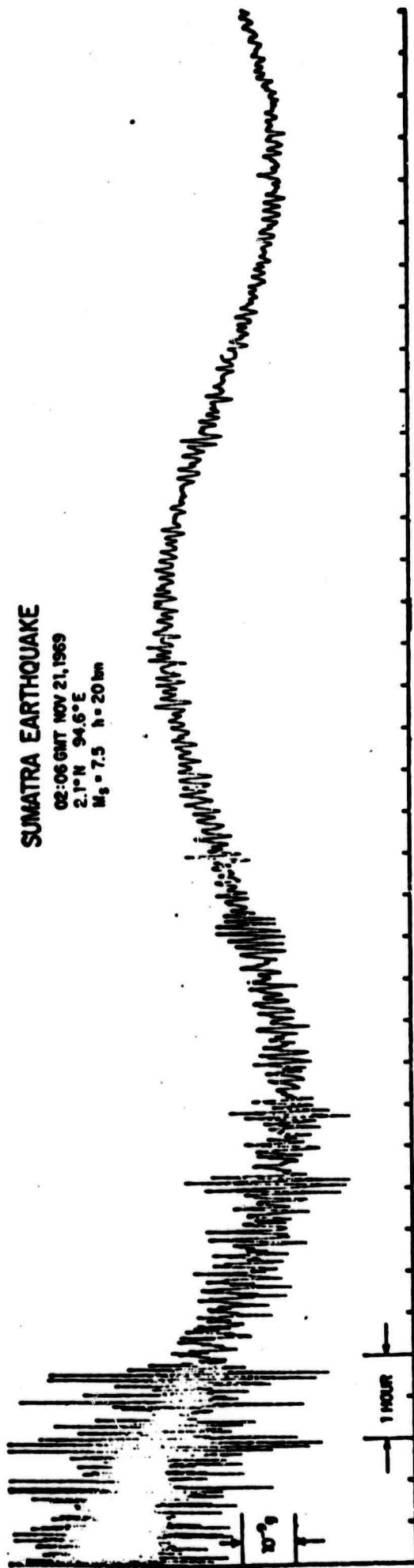
1 HOUR

10^{-6} g
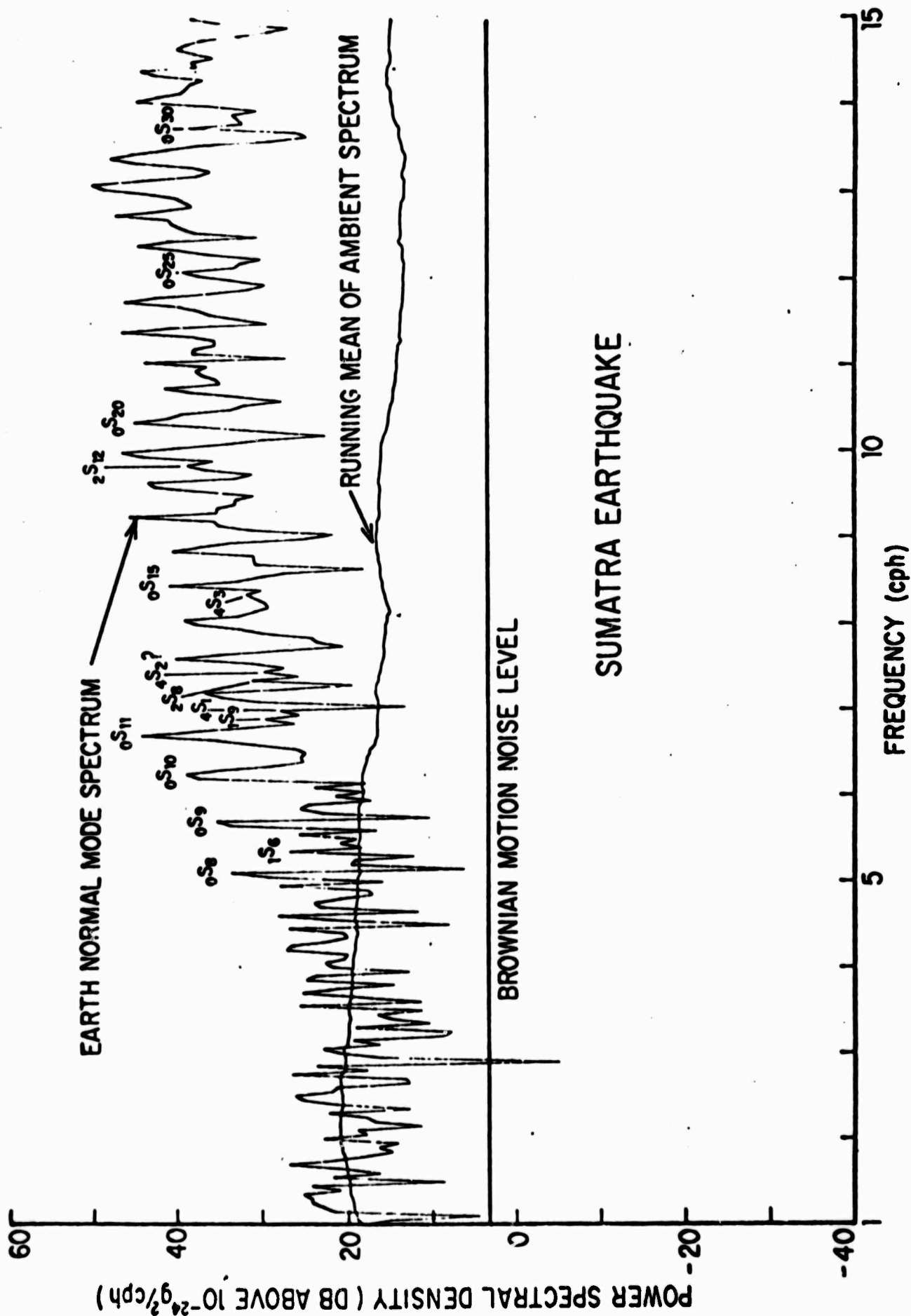
Figure 8

32
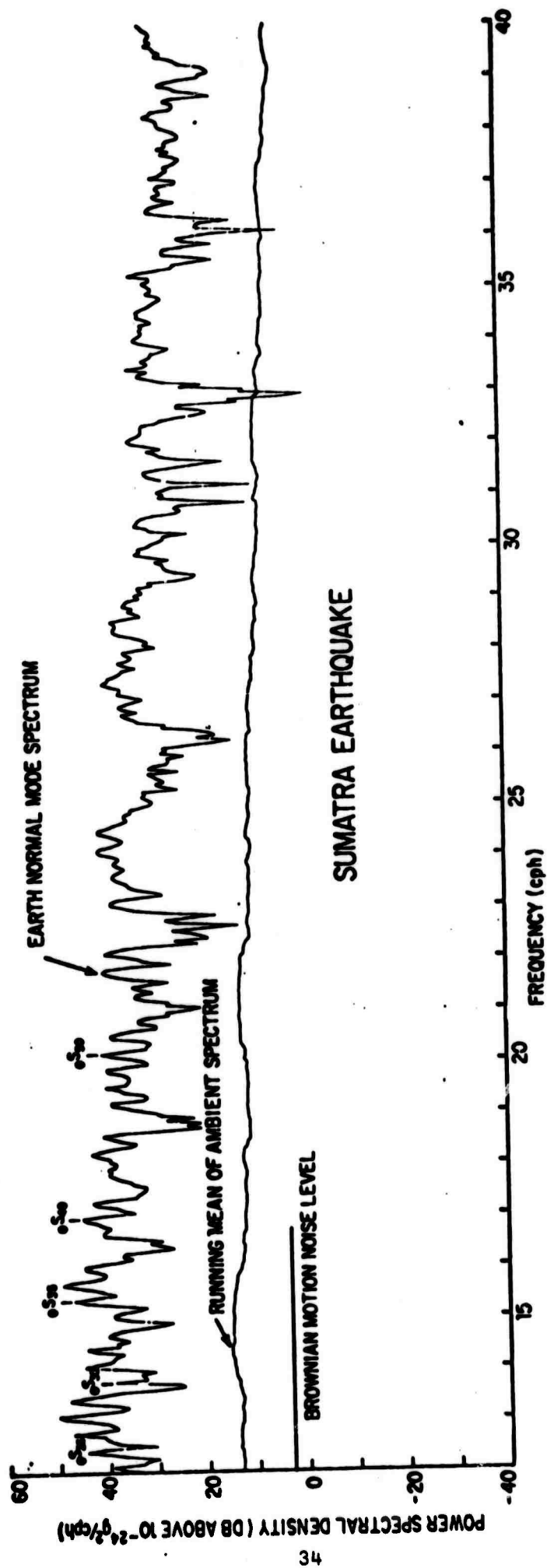
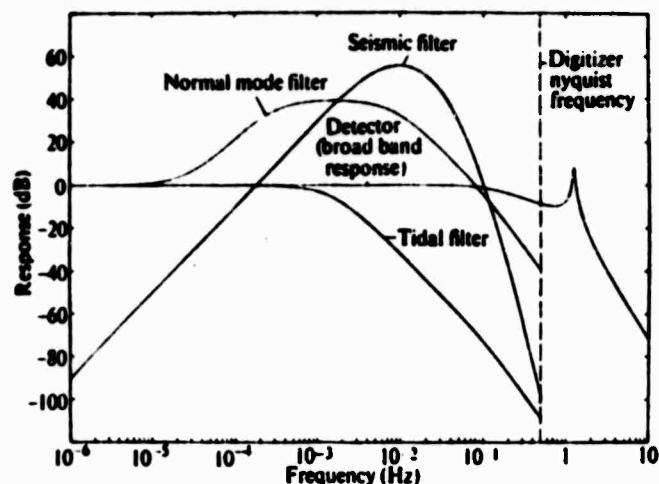SUMATRA EARTHQUAKE

Figure 9

33

Figure 10

Fig. 1 Acceleration response of various outputs of broadband accelerometer. The basic broadband response is that at the detector output. The other curves show the response when the detector output is passed through three analogue filters. The graph shows the response for the vertical accelerometer. The horizontal responses are the same, except that the resonance peak is slightly shifted and the relative gain of the seismic filter is slightly different. The zero dB point is 6.3×10^6 V/g for the vertical instrument, 1.95×10^6 (V/g or V rad^{-1}) for the horizontal, and 2.83×10^6 (V/g or V rad^{-1}) for the horizontal seismic filter.

It has a natural period of 0.807 s and a Q of 21. The horizontal accelerometer is of essentially similar design. In this instrument, a simple pendulum 24 cm in length, with a mass of 23 g, hangs vertically from the quartz fibre. The fibre stores the energy in the vertical accelerometer, but in the horizontal it acts chiefly as a loss-free pivot. Nearly all the energy is stored in the gravitational field, so that the natural period is the pendulum period. The results here were obtained with an instrument whose natural period is 0.91 s and whose Q is 20.

The instruments discussed here are of relatively small size and feature internal control of temperature and pressure[3]. They

Teleseismic Detection with Wide Band Vertical and Horizontal Accelerometers

THE observation of distant seismic events using a wide-band vertical accelerometer has recently been reported[1]. This is a preliminary report of the observation of teleseisms with both the vertical accelerometer and a new wide-band horizontal accelerometer at a surface site. Previous surface measurements of teleseisms with horizontal seismometers have been complicated by high levels of instrument and ground noise[2]. With present instrumentation and the aid of simple digital filtering, it is possible to obtain signal-to-noise ratios for a horizontal instrument at the surface comparable to those for the vertical instrument. In fact, if Love waves are produced, the signal-to-noise ratio for the surface horizontal accelerometer often exceeds that for the vertical.

The vertical accelerometer, which has been described in detail already[3], uses a quartz fibre held in torsion by a mass of 9.5 g.
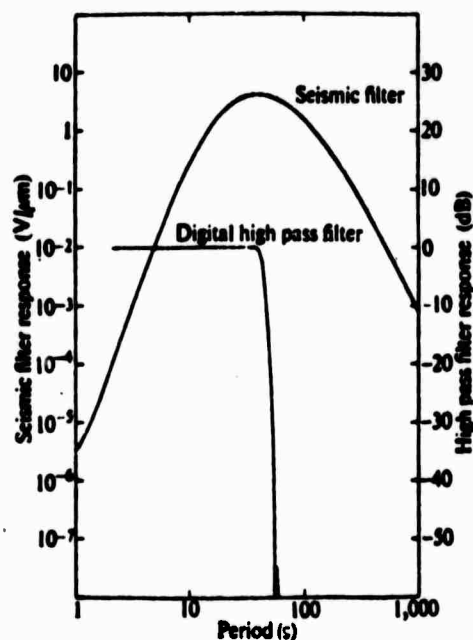

Fig. 2 Response to ground displacement at seismic filter output of vertical accelerometer (scale at left) and response of digital high pass filter (scale at right). The seismic filter output for the horizontal instrument is not readily interpreted in terms of ground displacement. The small bump in the response of the high pass filter is the first sideband. The response of the high pass filter is essentially unity at periods shorter than 45 s.

Fig. 3 High-resolution computer
plots from digitized records of
horizontal and vertical seismic filter
outputs. Traces *a* and *b* show the
raw outputs of the seismic filters
for the horizontal and vertical
accelerometers, respectively. Traces
c and *d* show the seismic filter
outputs from the horizontal and
vertical instruments after applica-
tion of the digital high pass filter
of Fig. 2. Although the scale
is the same for all the traces in
Figs. 3–6, the equivalent accelera-
tion response of the horizontal
seismic filter is lower than that
of vertical by a factor of 2.2 (see
text).
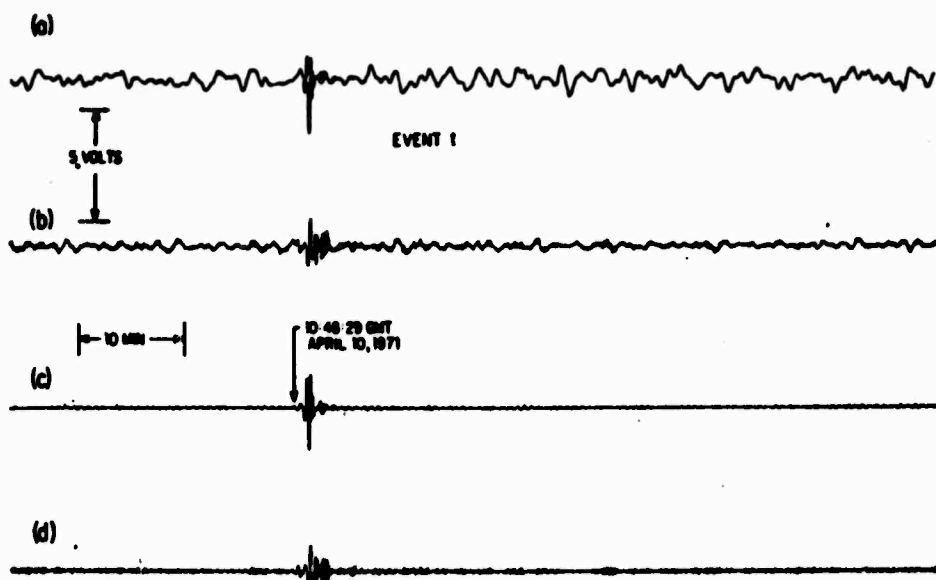
measure 9 inches in outer diameter, the horizontal instrument
being slightly longer than the vertical. Internal environmental
control allows for deployment without elaborate vault prepa-
ration. Both instruments are suitable for deployment in bore
holes.

Both the vertical and horizontal instruments use capacitative
position sensors and phase sensitive detection[3]. Their response
to acceleration is flat from d.c. to the natural resonance fre-
quencies of the mass-fibre systems. As the natural resonance
frequencies are greater than 1 Hz, the bandwidth of flat
response is from d.c. to about 1 Hz for both instruments. For
geophysical and seismic observations, the output of the phase-
sensitive detector is passed through any of three analogue
filters: a tidal filter, a normal mode filter, and a seismic filter.
Fig. 1 shows the broadband response of the vertical accelero-
meter at the detector output and at the outputs of the three
filters. The curves are normalized to the d.c. response at the
detector output. For the horizontal accelerometer the
responses are quite similar, except that there is a slight shift in
the frequency of the resonance peak and a different relative
normalization of the seismic filter output.

The d.c. gain of each instrument at the detector output, which
is taken as unity in Fig. 1, has been carefully measured. For
the vertical accelerometer, it has been determined by tilt
calibration and by a fit of the theoretical Earth tides to the
tidal filter output. The result is

$$G_v = (6.25 \pm 0.1) \times 10^6 \text{ volts}/g$$

where g is the local acceleration of gravity. At this gain,
peak-to-peak tidal acceleration, or about $3 \times 10^{-7}g$, amounts
to one tenth of the full scale range of ± 10 V at the detector
output. For the horizontal instrument, the d.c. gain at the
detector output has been determined by tilt calibration and
checked against design calculations. It is

$$G_h = (1.95 \pm 0.1) \times 10^6 \text{ volts}/g$$

Although data from all three analogue filters are continuously
recorded for both instruments, we show here only data from
the seismic filters, which were designed to match the response
of a long-period seismometer. Fig. 2 shows the response of
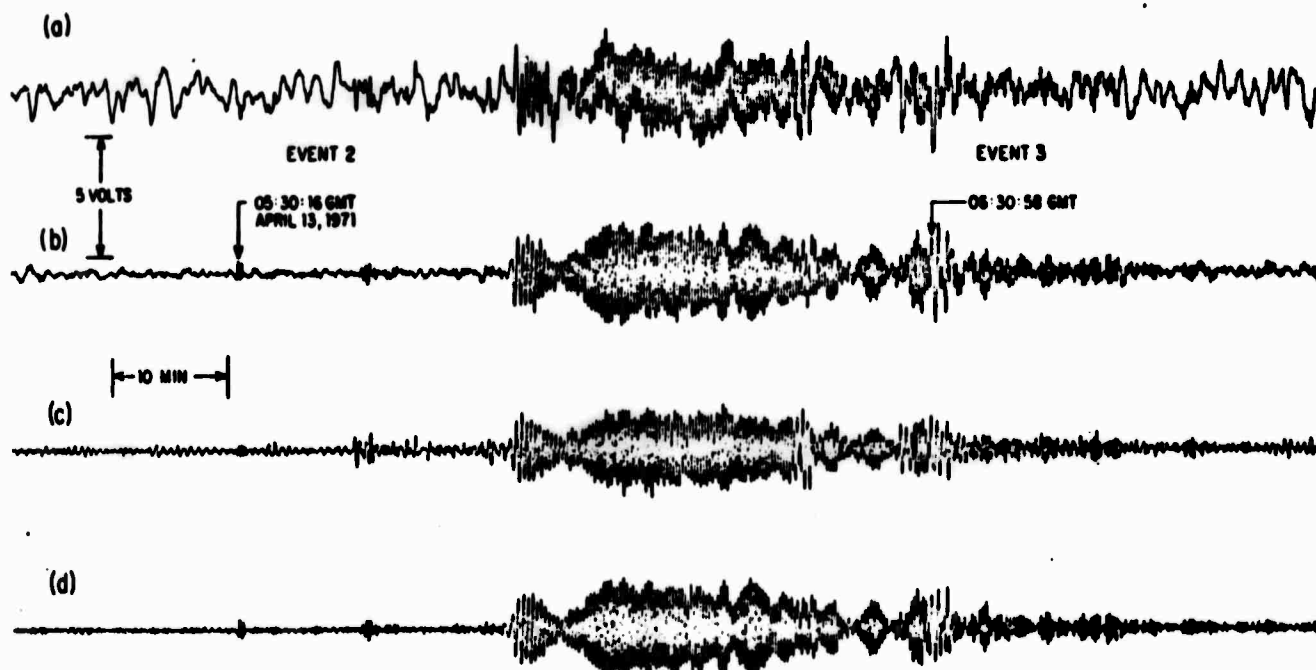the vertical accelerometer to ground displacement at the seismic
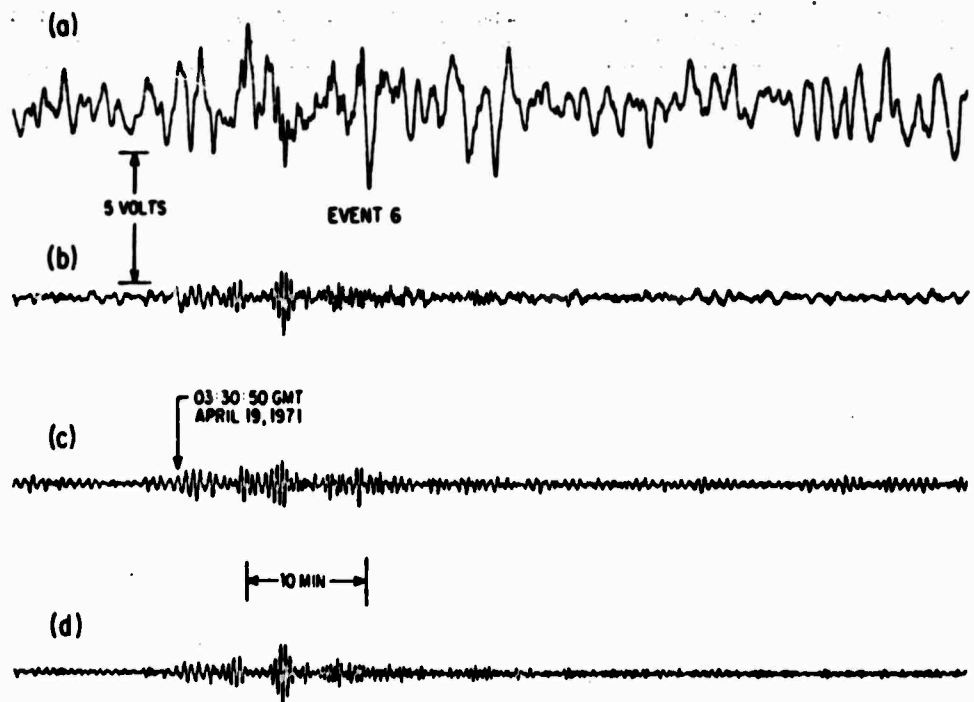

Fig. 4 See caption to Fig. 3.

(a)

5 VOLTS   EVENT 6

(b)

Fig. 5 See caption to Fig. 3.

(c)

03 30 50 GMT
APRIL 19, 1971

|—10 MIN—|

(d)

filter output. It is computed using the standard seismic approximation in which only kinematic acceleration is considered. As the horizontal instrument measures both kinematic acceleration and tilt, interpretation in terms of ground displacement is not possible for it. The response at its seismic filter output is best obtained from Fig. 1.

Due to a difference in the attenuators at the two seismic filter outputs, 0 dB for the horizontal seismic filter in Fig. 1 is 2.83×10^5 volts per g of acceleration or per radian of tilt. For all the other outputs of the horizontal, 0 dB is 1.95×10^6 volts/g as before. Thus, for the seismic filter output, the equivalent acceleration response of the horizontal instrument is a factor of 2.2 less than that for the vertical.

The two instruments operate side by side at a surface site (vault depth of 10 feet) at the University of California Elliott Field Station (32.88° N, 117.1° W). The horizontal instrument is oriented N 45° E for future comparison with a laser strain

meter[4] at the same site. All the filter outputs for both instruments are recorded digitally on magnetic tape at a sampling interval of 1 s. At this sampling rate, each filter provides sufficient attenuation at the digitizer Nyquist frequency of 0.5 Hz to avoid aliasing (see Fig. 1).

The upper two traces of Figs. 3 to 6 are high resolution computer plots taken from the digitized seismic filter data from both instruments. Trace a is the horizontal seismic filter output, and trace b the vertical. The figures show the noise levels at various times of night, as well as five distant earthquakes.

Careful inspection of these records shows that the noise from the horizontal instrument is concentrated at frequencies slightly below those of seismic interest. In fact, most of the horizontal noise can be removed from the records by digital filtering. The lower two traces in Figs. 3 to 6 show the result of the application of a high pass convolution filter to the data
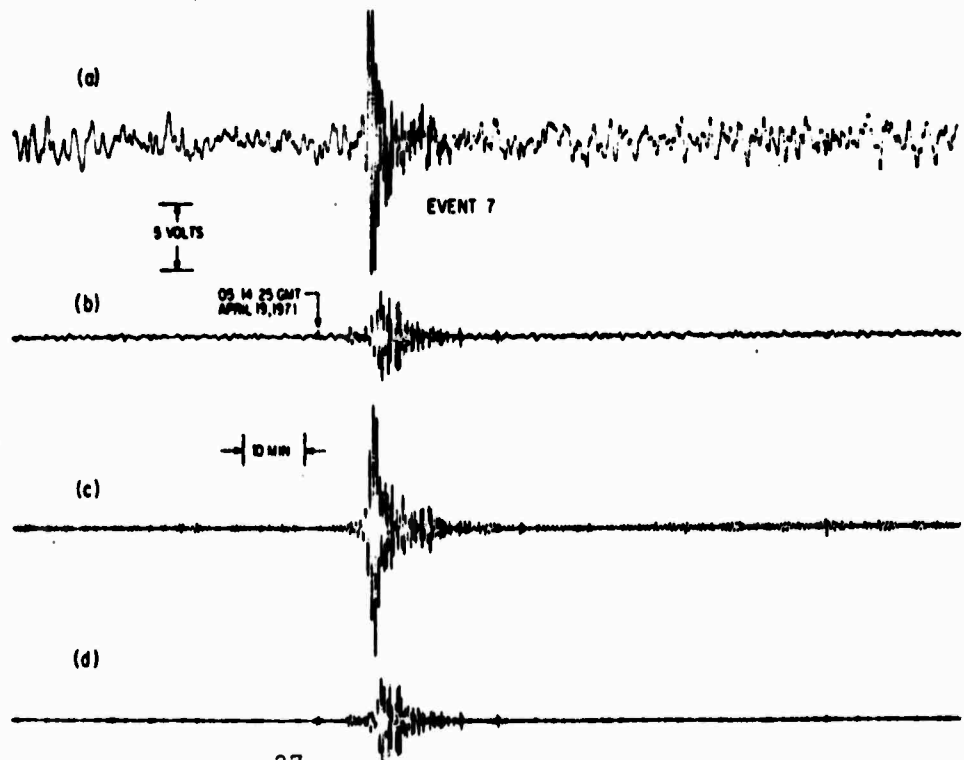

(a)

5 VOLTS   EVENT 7

(b)

05 14 25 GMT
APRIL 19, 1971

Fig. 6 See caption to Fig. 3.

—| 10 MIN |—

(c)

(d)

37

of the upper two traces. This high pass filter, whose response is shown in Fig. 2, has a −3 dB breakpoint at a period of 45 s and is down 20 dB at 50 s. After digital filtering, the peak-to-peak horizontal noise (trace c) is reduced by nearly an order of magnitude, yet the seismic signal is unaffected by the filtering. The signal-to-noise ratio for the vertical record is also improved by digital filtering, as shown in trace d.

Although the site is subject to acoustic and ground noise from planes and a jet engine testing facility at the nearby Miramar Naval Air Station, noise in the seismic band is relatively low, at least for the vertical instrument. The horizontal noise, however, is much higher and varies with weather and the time of day. If the output of the horizontal instrument is interpreted in terms of acceleration, and if the difference in d.c. gain between the two instruments is taken into account, the vertical and horizontal noise levels can be compared. At night, the horizontal noise is a factor of six to fifteen greater in equivalent acceleration than the vertical. During midday, this factor is augmented by as much as another factor of three, especially during windy and variably cloudy days. When the weather is calm and uniformly overcast, as on foggy days, the daytime horizontal noise is as low as at night. The horizontal noise is due chiefly to ground tilt induced by short-range pressure and temperature fluctuations[2-5].

mental conditions, lead us to believe that the observed noise is predominantly real motion of the Earth.

There are several features of interest in the events observed. Table 1 gives the identification and parameters of the events, all of which occurred during the period April 10 to 19, 1971. The angle α is the smallest angle between the great circle path connecting the epicentre to the station and the line of maximum sensitivity of the horizontal instrument. When this angle is near 90°, only transversely polarized Love waves are observed by the horizontal instrument. When it is close to zero, only Rayleigh waves, which are longitudinally polarized, are seen.

Event 1 had an angle α of 80°, and strong Love wave arrivals were observed. The signal-to-noise ratio on the digitally filtered record from the horizontal instrument was nearly 20 for this event of body wave magnitude 4.1 at a distance of 10°. Even after digital filtering, the signal-to-noise ratio on the vertical instrument was only eight. This pattern of high horizontal signal-to-noise is repeated in event 7, which also showed strong Love waves. Event 7, an earthquake of body wave magnitude 4.9 at 44°, had a signal-to-noise ratio greater than thirty on the digitally filtered horizontal record.

Events 2, 3, and 6 are examples of earthquakes whose seismic waves arrived along the line of maximum sensitivity of the horizontal instrument. For these events, Rayleigh waves

---

Table 1 Events Shown in Figs. 3 to 6

Event	Day (GMT)	Origin time (GMT)	Location	Epicentre	Mag. m_b	Mag. M_s [*]	Mag. M_s (30°)[†]	Depth (km)	Distance Δ (deg)	Angle α [‡] (deg)	Source
1	April 10, 1971	10:45:40	Baja California	24.8° N, 111.0° W	4.1	3.0	3.8	33	10	80	LASA[§]
2	April 13, 1971	05:17:58	Tonga Island region	22.8° S, 175.4° W	5.0	5.0	4.3	33	78	8	LASA
3	April 13, 1971	05:57:34.5	Tonga Island region	15.9° S, 174.0° W	5.5	4.5	3.9	73	73	13	NOAA PDE[¶]
6	April 19, 1971	02:43:52.2	Greece–Albania border region	39.0° N, 20.3° E	5.1	4.5	3.7	16	98	13	NOAA PDE
7	April 19, 1971	05:05:25	Galapagos Island region	2.3° S, 89.6° W	4.9	4.6	4.4	17	44	87	LASA

[*] The surface wave magnitude M_s is computed from the Gutenberg formula $M_s = \log_{10} A + 1.66 \log_{10} \Delta + 1.82$, where A is the maximum zero-to-peak amplitude of ground displacement in μm measured for seismic waves with periods near 20 s.

[†] The surface wave magnitude M_s (30°) is the magnitude of a hypothetical earthquake at $\Delta = 30°$ which would produce a signal of the same amplitude as that of the given event.

[‡] Angle α is the smallest angle between the great circle path from epicentre to station and a line running 45° east of north (the line of maximum sensitivity of the horizontal instrument).

[§] LASA = Large Aperture Seismic Array in Montana.

[¶] NOAA PDE = National Oceanographic and Atmospheric Administration—Preliminary Determination of Epicentres.

Noise originating in the instrument electronics has been measured by removing the reference signal at the phase-sensitive detector. The seismic filter output for either instrument with no reference is a straight line on the scales of any of Figs. 3 to 6. Calculations of the output noise due to the effects of Brownian motion on the mass and pendulum have been made. The power spectral density of fluctuations at the detector output due to Brownian motion is about 3×10^{-7} V^2 Hz^{-1} for the vertical instrument and about 1×10^{-8} V^2 Hz^{-1} for the horizontal. The horizontal Brownian noise is lower than the vertical because of the larger mass of the moving system and the smaller gain. At the output of the seismic filter, the effect of Brownian motion is a fluctuation with an r.m.s. amplitude of 18 mV for the vertical and 3.5 mV for the horizontal. As Figs. 3 to 6 show, this is at least an order of magnitude down from the noise amplitudes observed. When a second horizontal accelerometer of this type is constructed, coherence will be measured to determine total instrumental noise levels. At present, the preliminary noise measurements and calculations, as well as the variation of the horizontal noise with environ-

were observed on both instruments. Fig. 4 of event 2 shows the characteristic Rayleigh wave dispersion on all four traces. Under the assumption that the horizontal signal derives entirely from kinematic acceleration and not from tilt, Fig. 4 can be used to estimate the polarization ratio for Rayleigh waves. When the difference in gain between the two instruments is taken into account, the polarization ratio (horizontal-to-vertical equivalent acceleration) for Rayleigh waves of 20 s period is found to be about 2.6. In general, the signal-to-noise ratio for Rayleigh waves is a factor of two better on the vertical, even after digital filtering.

Although the new wide-band horizontal accelerometer is noisy at this surface site, the noise is not in the frequency region of seismic interest. It can be removed by digital filtering. The digitally filtered horizontal records then become a powerful adjunct to the vertical records for purposes of seismic detection. Both the theoretical power of Love waves as a source discriminant and an augmented signal-to-noise ratio for events producing Love waves are now available.

We thank C. W. Van Sice for assembling the horizontal

BARRY BLOCK
JAY DRATLER, JUN.

Institute of Geophysics and Planetary Physics,
Scripps Institution,
PO Box 109,
La Jolla, California 92037

[1] Prothero, W., Dratler, J., Brune, J., and Block, B., *Nature Physical Science*, 231, 80 (1971).
[2] Capon, J., *J. Geophys. Res.*, 74, 3182 (1969).
[3] Block, B., and Moore, R. D., *J. Geophys. Res.*, 75, 1493 (1970).
[4] Berger, J., and Lovberg, R. H., *Science*, 170, 296 (1970).
[5] Haubrich, R. A., *Monographies de l'UGGI* (in the press).